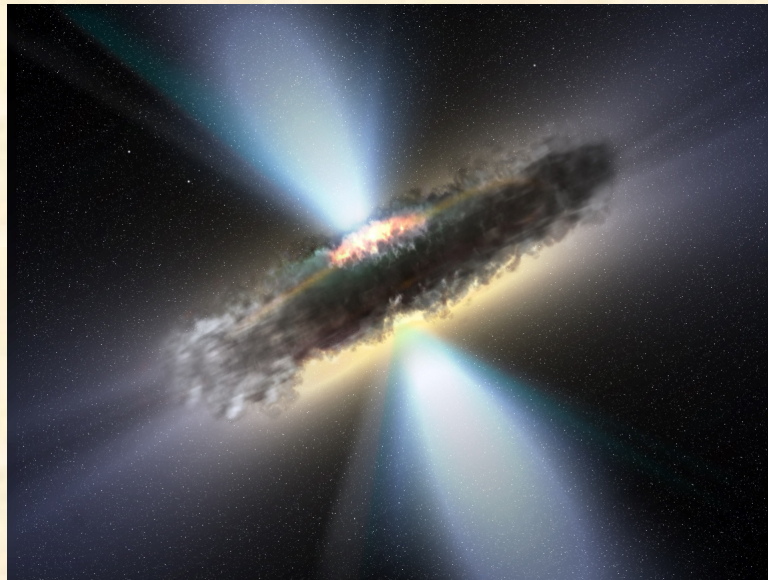


AGN Components

- Observed Components and Interpretation
- Dependence on AGN Type
- Continuum Emission Regions
- Emission-Line Regions



Seyfert 1



NLR

$d = 1 - 1000 \text{ pc}$
 $n = 10^2 - 10^6 \text{ cm}^{-3}$

BLR

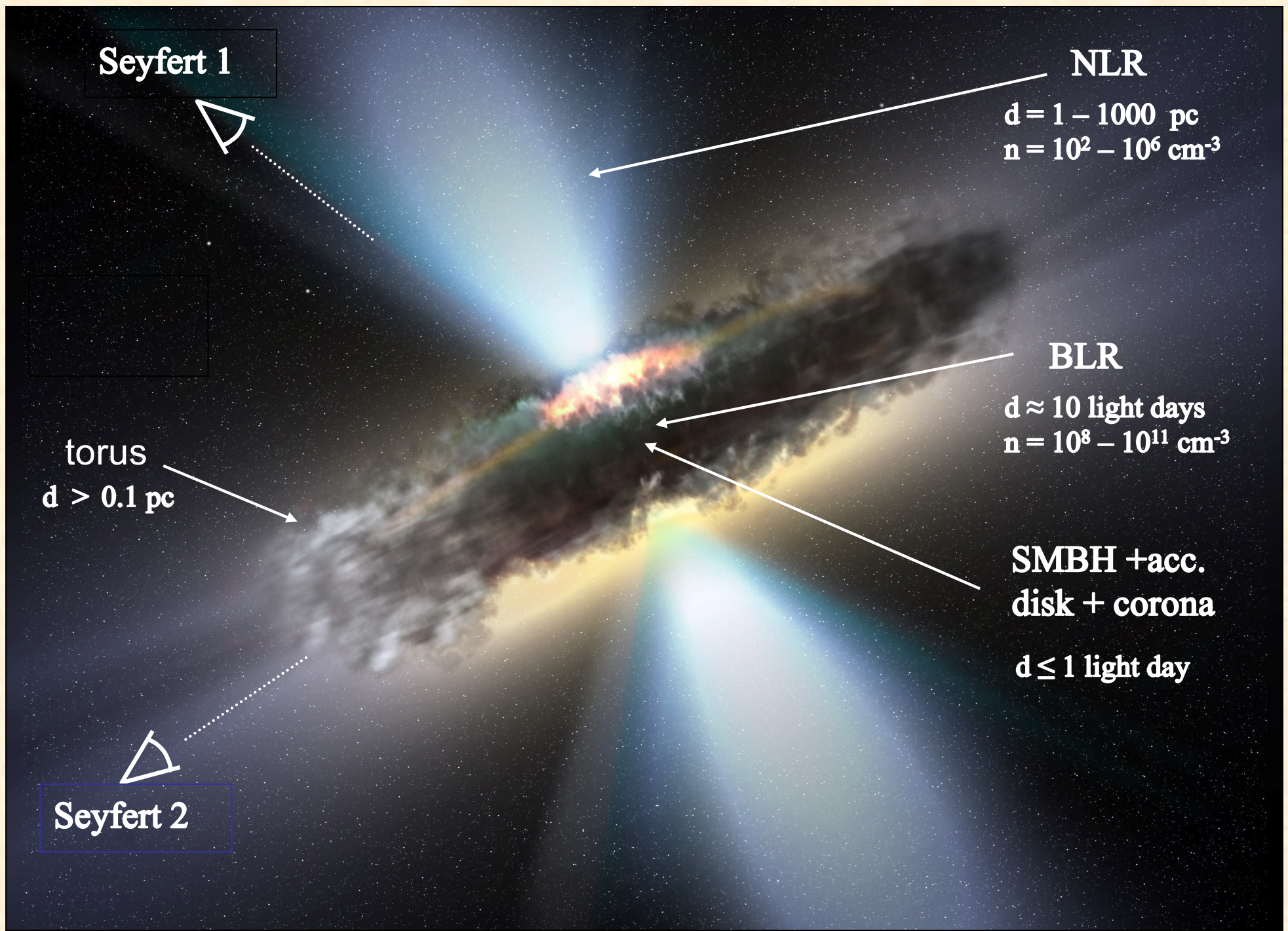
$d \approx 10 \text{ light days}$
 $n = 10^8 - 10^{11} \text{ cm}^{-3}$

SMBH + acc.
disk + corona

$d \leq 1 \text{ light day}$

torus
 $d > 0.1 \text{ pc}$

Seyfert 2



Observed Components of AGN

(and probable physical components)

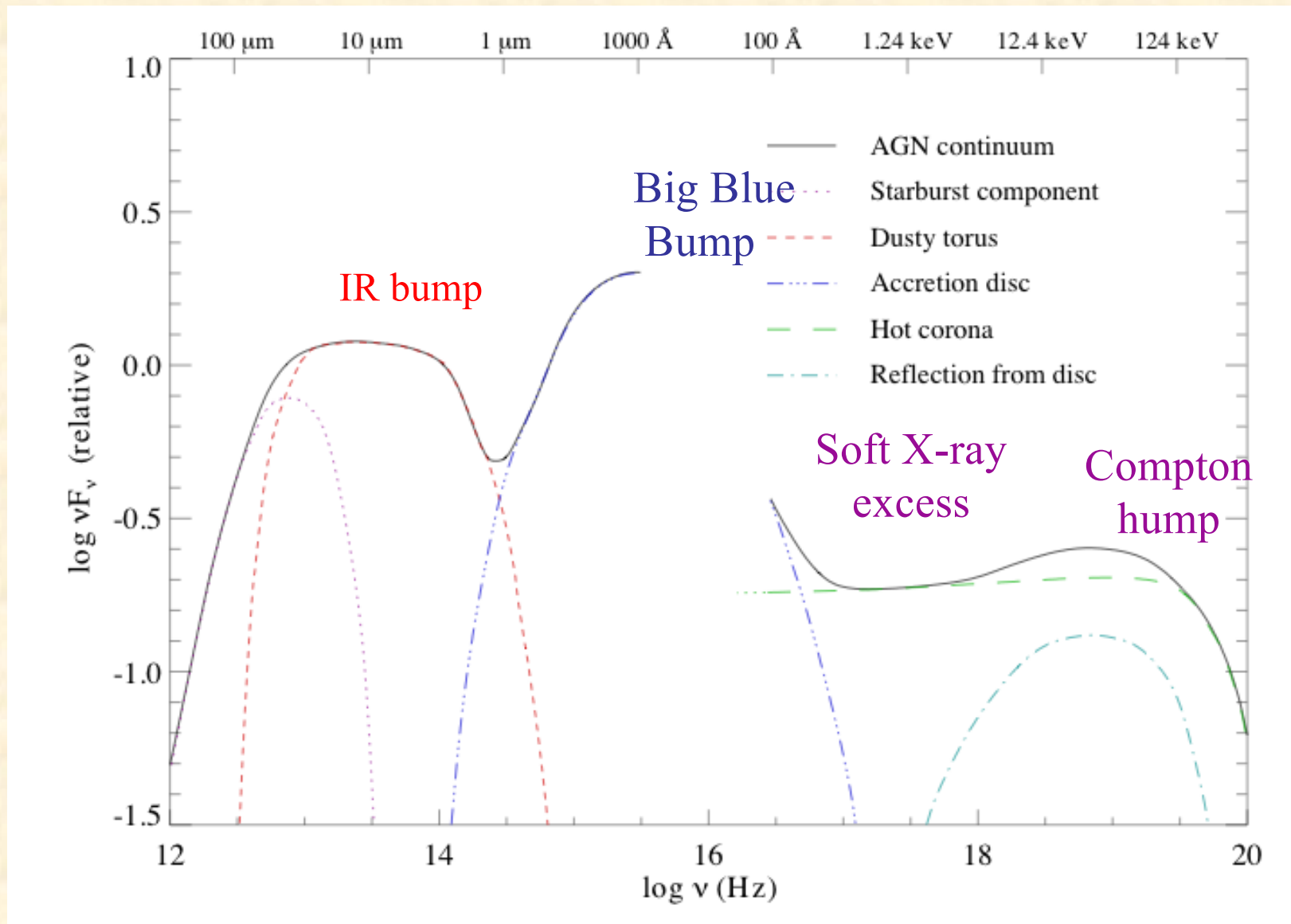
Spatially Unresolved:

- Optical/UV/soft X-ray continuum → accretion disk
- Hard X-ray continuum ($E > 1$ keV) → hot X-ray corona
- IR thermal emission → dusty torus (barely resolved in a few nearby sources), NLR dust
- Broad emission lines → broad-line region (BLR)
- Intrinsic UV/X-ray absorption lines → mass outflows

Spatially Resolved:

- Radio emission → core, jets, lobes
- Narrow emission lines → narrow-line region (NLR)
- Ionized gas in the host galaxy → extended narrow-line region (ENLR)

Schematic Continuum SED for Seyferts



Characterization of Continuum SEDs

- Typically characterized by power-laws over a limited range in frequency (or wavelength):

$$F_\nu \propto \nu^{-\alpha_\nu} \quad (\text{larger } \alpha_\nu \rightarrow \text{"steeper" continuum})$$

$$\text{For } F_\lambda \propto \lambda^{-\alpha_\lambda} \rightarrow \alpha_\lambda = 2 - \alpha_\nu$$

X-ray folks tend to use photon flux (photons $\text{s}^{-1} \text{cm}^{-2} \text{keV}^{-1}$)

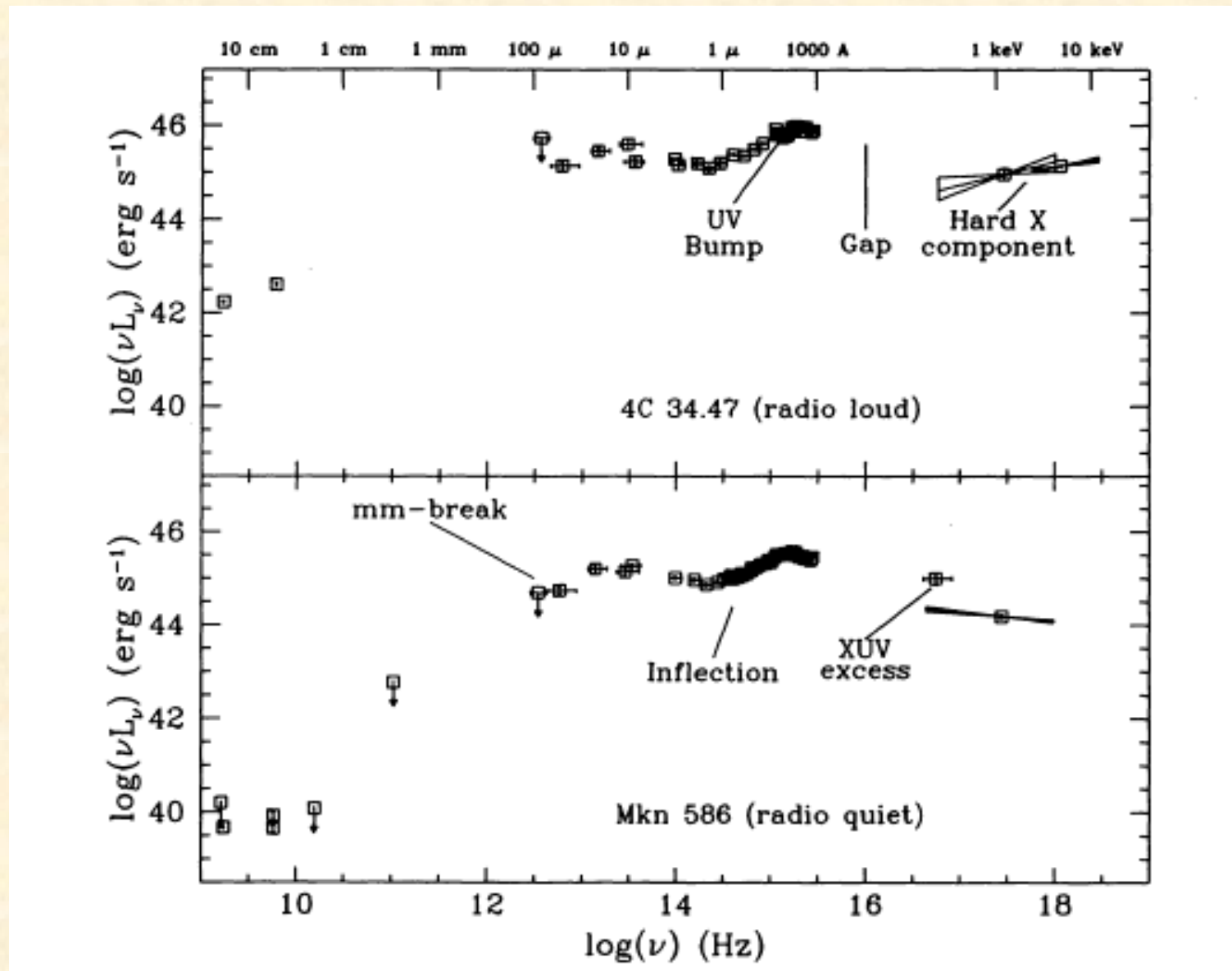
$$F_{\text{ph}} \propto E^{-\Gamma} \rightarrow \Gamma = \alpha_\nu + 1$$

- SED often plotted as νF_ν - represents energy output at each ν

$$\text{If } \alpha_\nu < 1 \rightarrow \nu F_\nu \propto \nu^{1-\alpha_\nu} \propto \nu^{\text{pos.}\#} \quad (\text{positive slope in } \nu F_\nu \text{ plot})$$

$$\text{If } \alpha_\nu > 1 \rightarrow \nu F_\nu \propto \nu^{1-\alpha_\nu} \propto \nu^{\text{neg.}\#} \quad (\text{negative slope in } \nu F_\nu \text{ plot})$$

Observed Quasar SEDs (Elvis 1994)



- Radio-quiet (RQ) quasars - similar to Seyfert 1s (EUV slightly steeper)
- Radio-loud (RL) quasars $\sim 100x$ brighter in radio than RQ

Continuum SEDs for Seyferts/Quasars

1) Optical/UV: $\alpha_v \approx 0.5$ to 1.0

Note: low luminosity AGN contaminated by starlight in optical

2) Soft X-rays ($E < 1 - 2$ keV): $\Gamma > 2$ (steep, "soft X-ray excess")

- however, often absorbed by MW and host galaxy hydrogen, torus

3) Hard X-rays ($E > 1 - 2$ keV): $\Gamma \approx 1.7$ (flat out to ~ 10 keV)

- Compton reflection (down-scattering) from disk: hump at $E > 10$ keV

4) EUV: Galaxy is optically thick to H-ionizing radiation - interpolate

Optical (2500 Å) to X-ray (2 keV): $\alpha_{ox} \approx 1.5$ (Quasars are steeper)

5) IR continuum: often fit with a combination of blackbodies (hot dust)

- dust sublimates at $T \approx 2000$ K, which leads to a minimum at $\sim 1 \mu\text{m}$

6) Sub-mm break: sharp drop to radio, $\alpha > 2.5$

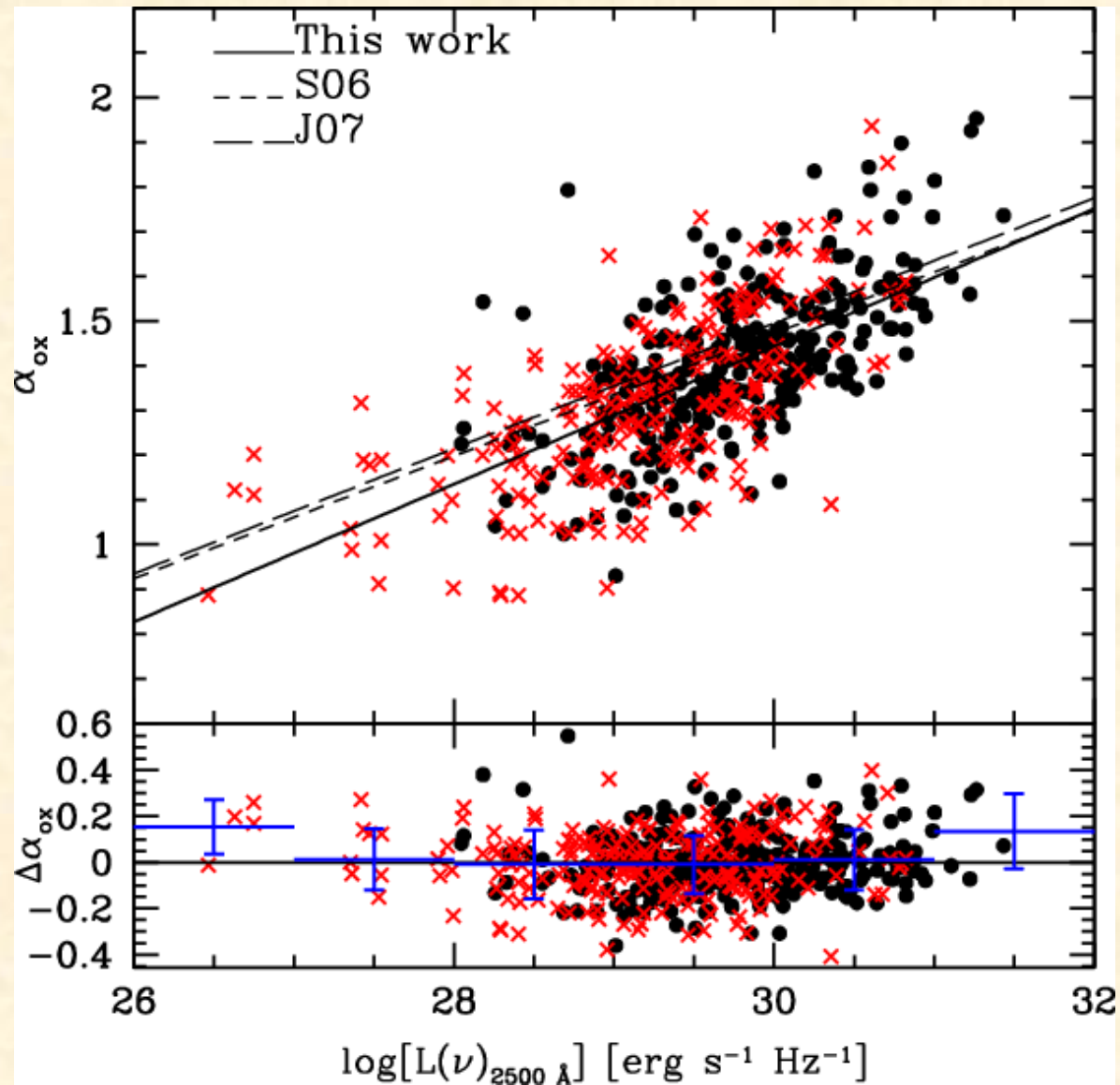
- probably synchrotron self absorption

7) Radio: very weak in Seyferts and RQ quasars

- VLBI detects weak, aligned radio blobs instead of relativistic jets

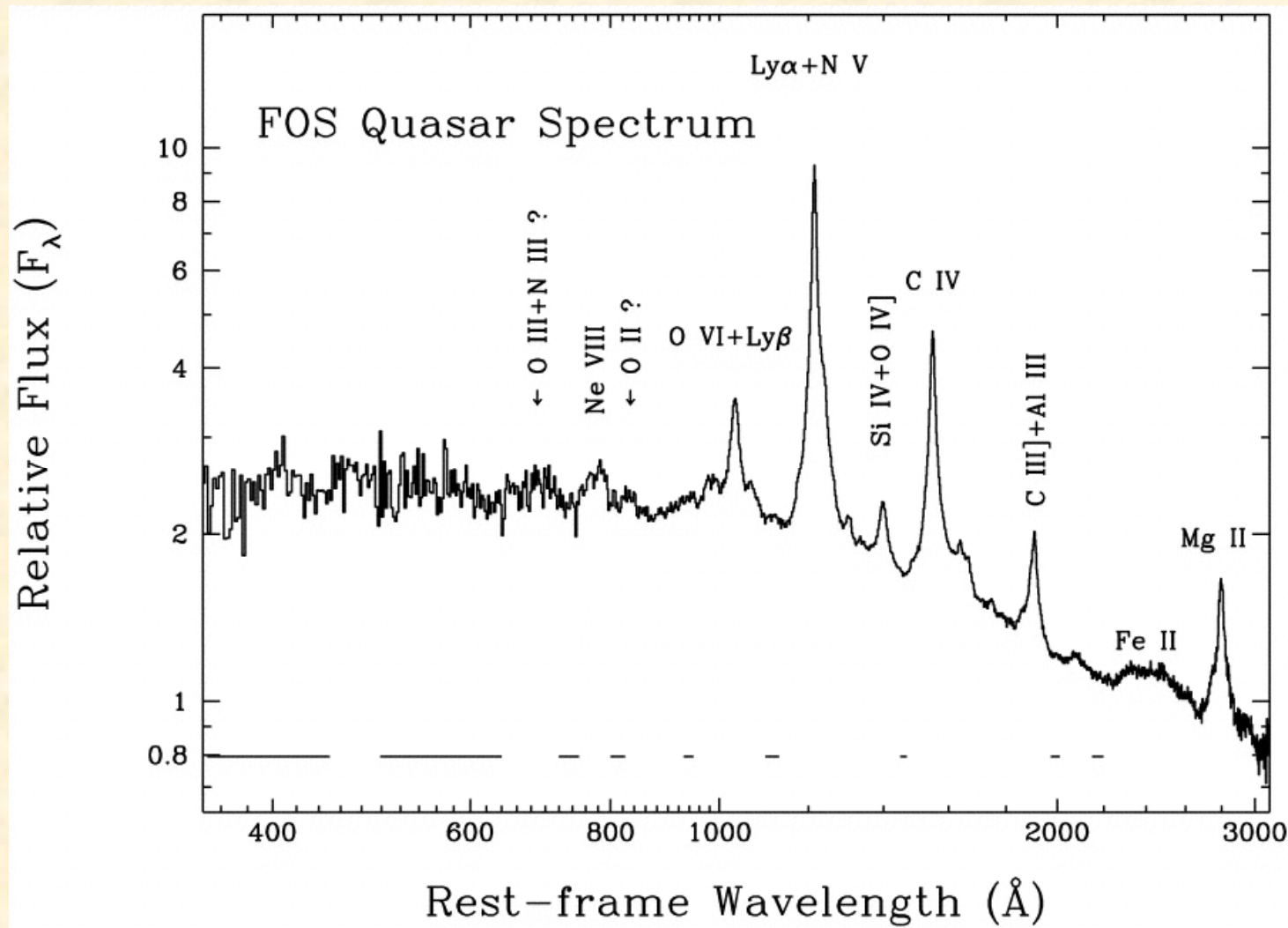
(RL AGN: $\alpha_v < 0.5$ - flat-spectrum (face-on), $\alpha_v > 0.5$ - steep spectrum)

Correlation of α_{ox} with Luminosity



(Lusso et al. 2010, A&A, 512, 34)

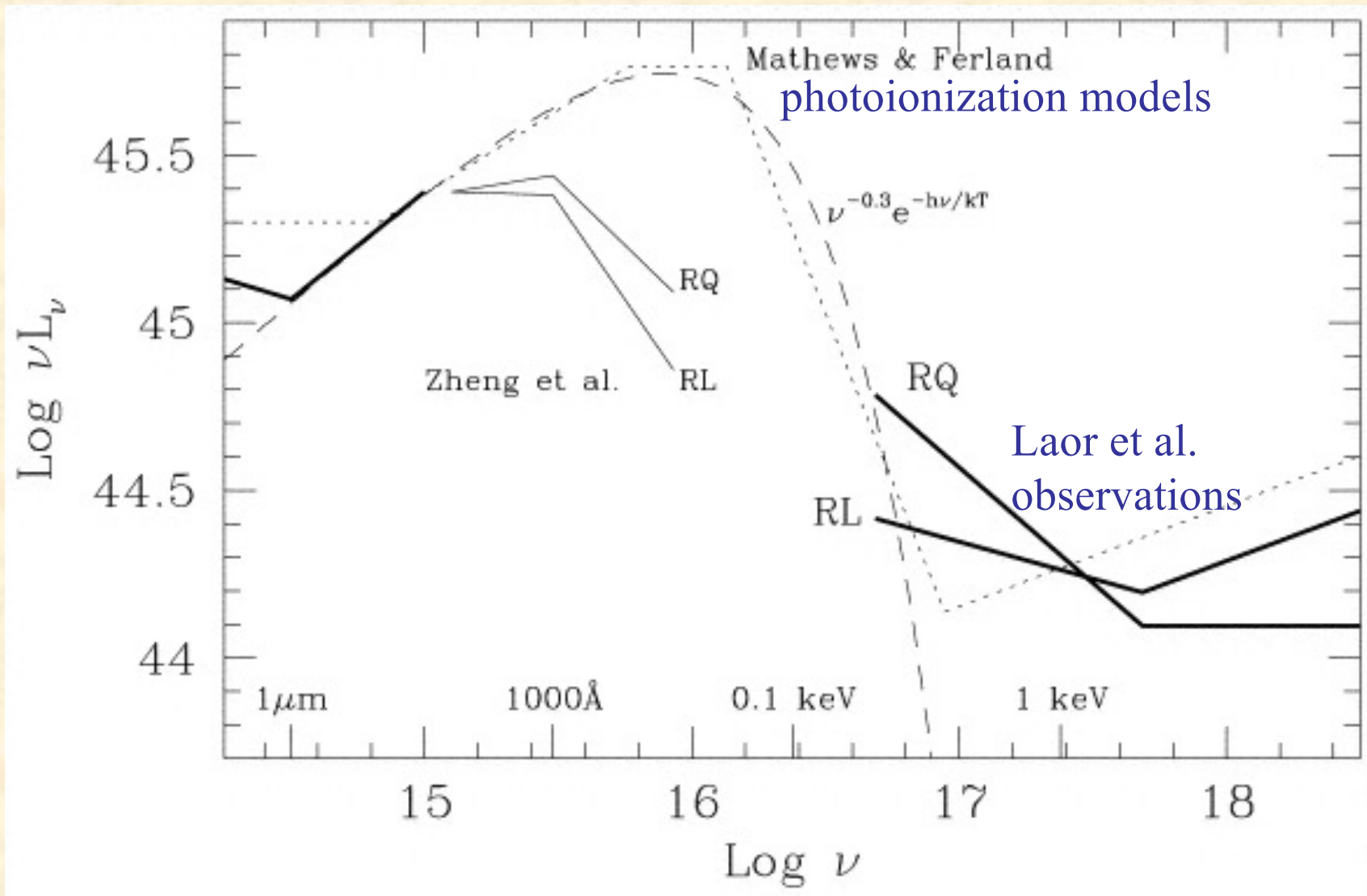
1) Optical/UV/EUV: The BBB and Accretion Disks



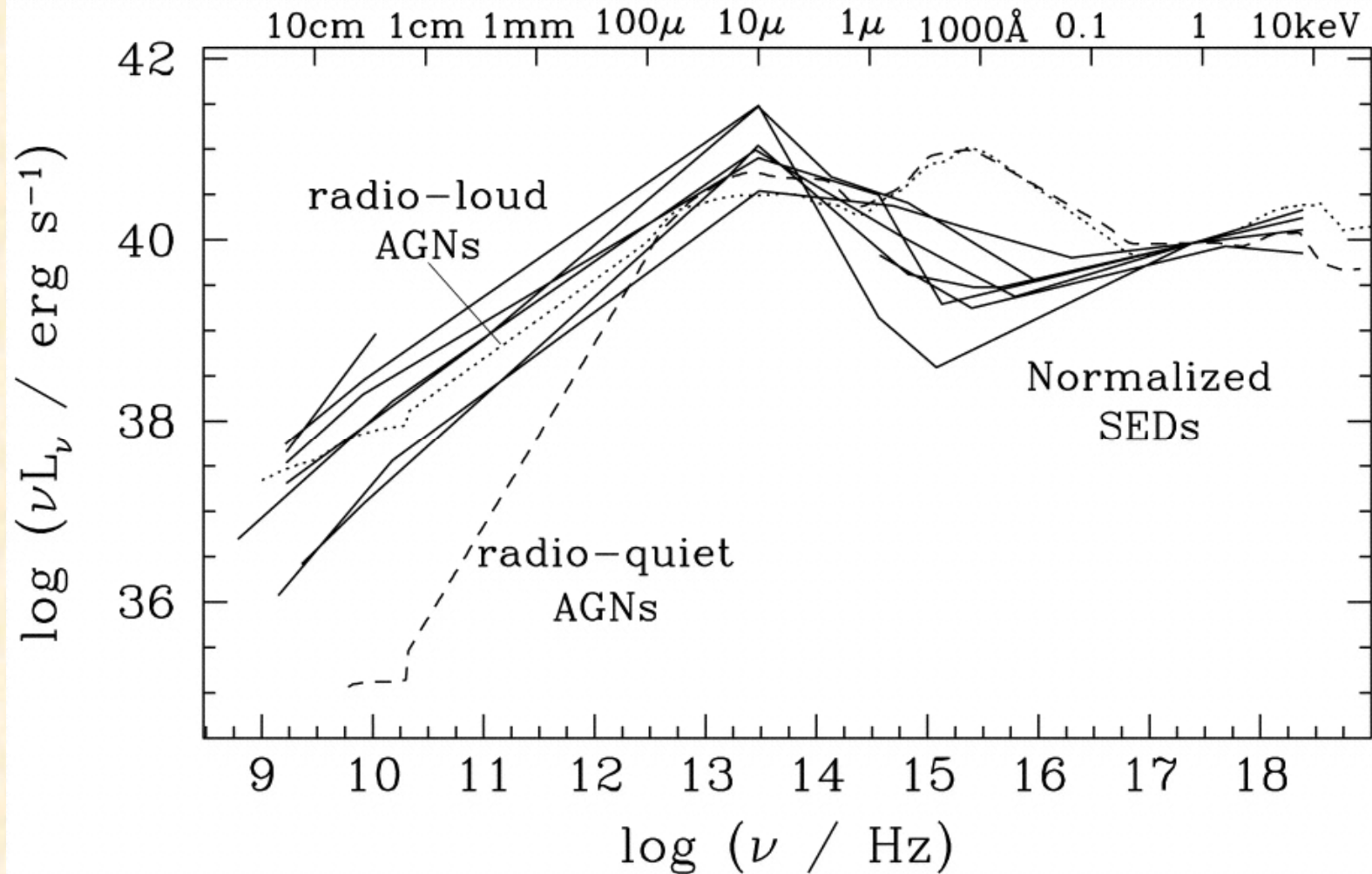
(Zheng, et al. ApJ, 475, 569)

- Composite spectrum from quasars at different z 's
- Turns over in EUV more quickly than previous predictions used in photoionization models (Mathews & Ferland 1987).

Big Blue Bump(BBB) - not so big? (Laor 1997)



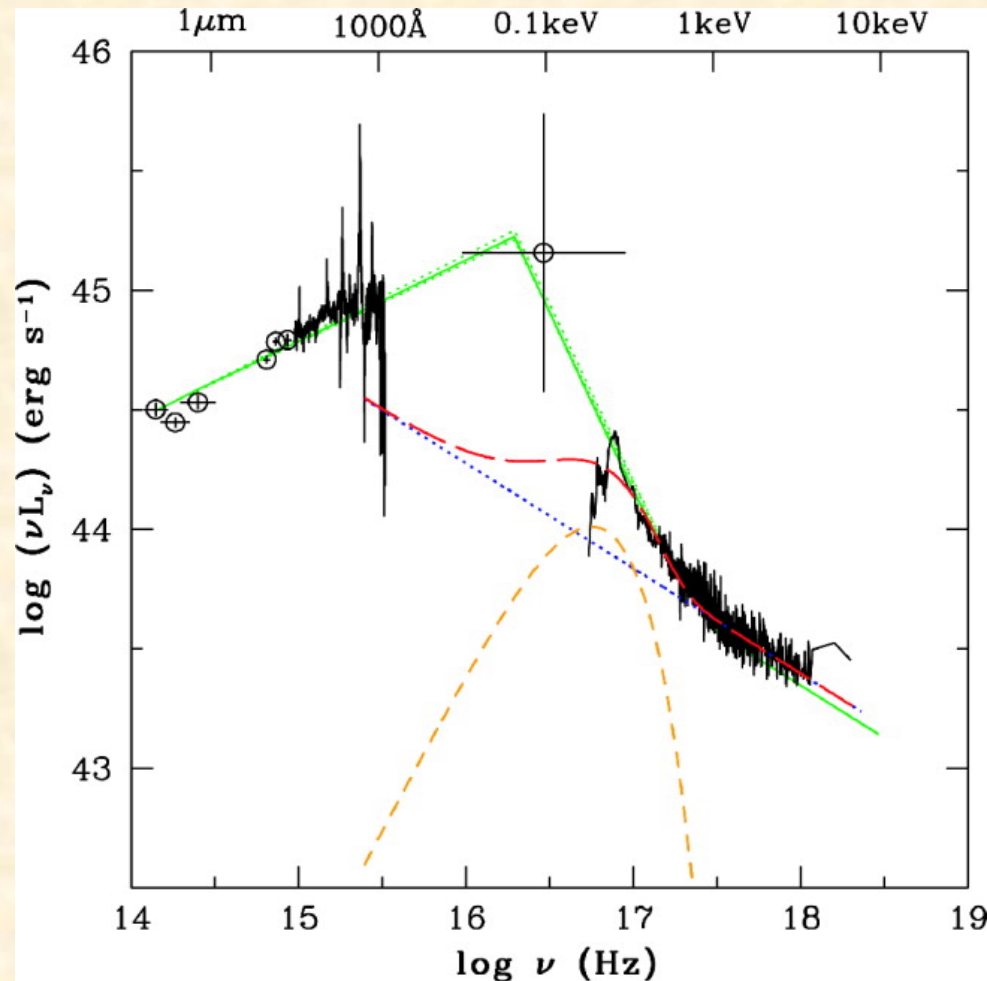
SEDs of LINERs (solid lines)



(Ho, 1999, ApJ, 516, 672)

- LINERs have weak or nonexistent BBBs, low L/L_E ($=10^{-5} - 10^{-3}$)
- Consistent with idea that their disks are ADAFs
- However α_{ox} similar to Seyferts (Maoz et al. 2007)

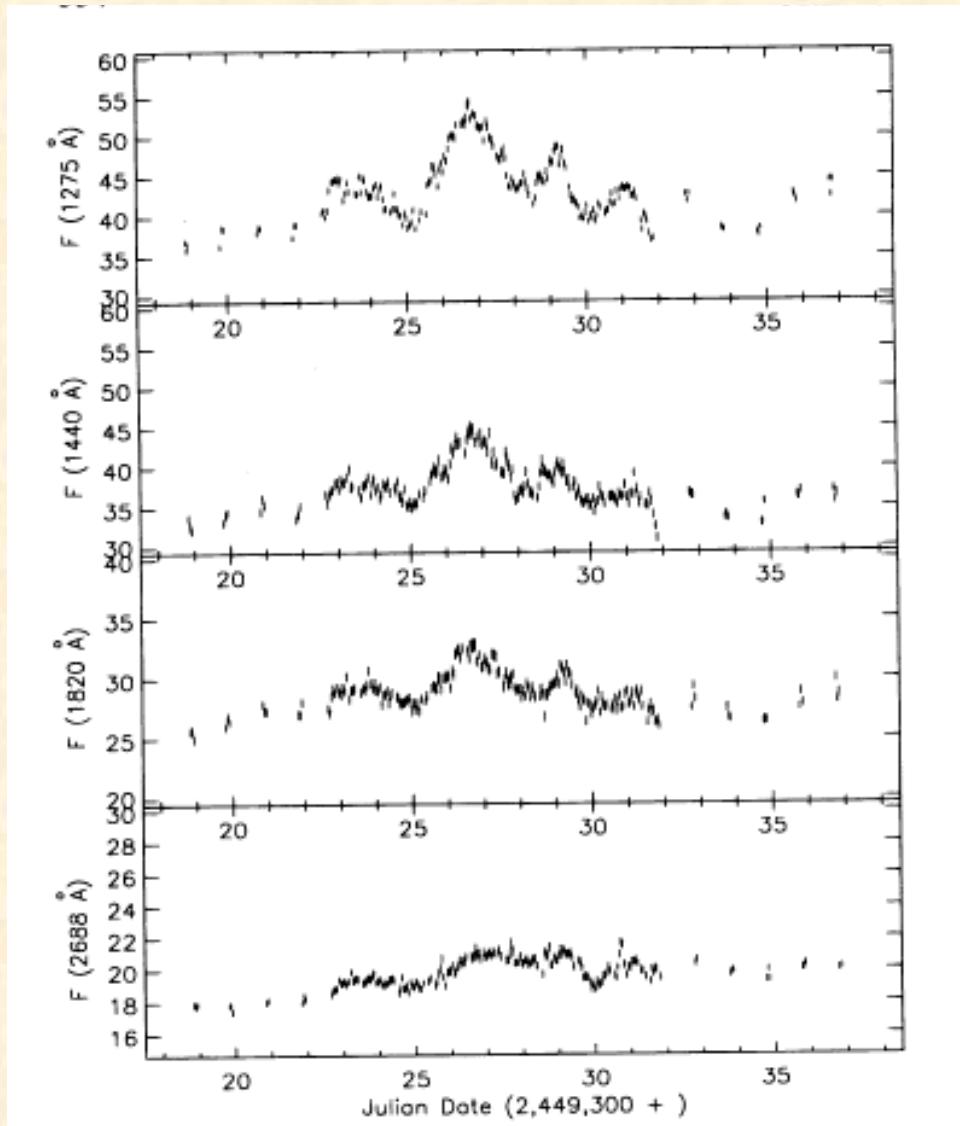
SEDs of NLS1s



(Turner, et al. 2002, ApJ, 568, 120)

- NLS1s may have stronger BBBs (Grupe et al. 2010, ApJS, 187, 64)
- Peak emission may be shifted to higher energies \rightarrow strong, soft X-ray excess
- Possibly due to high L/L_E ($=10^{-1} - 1$) in most NLS1s

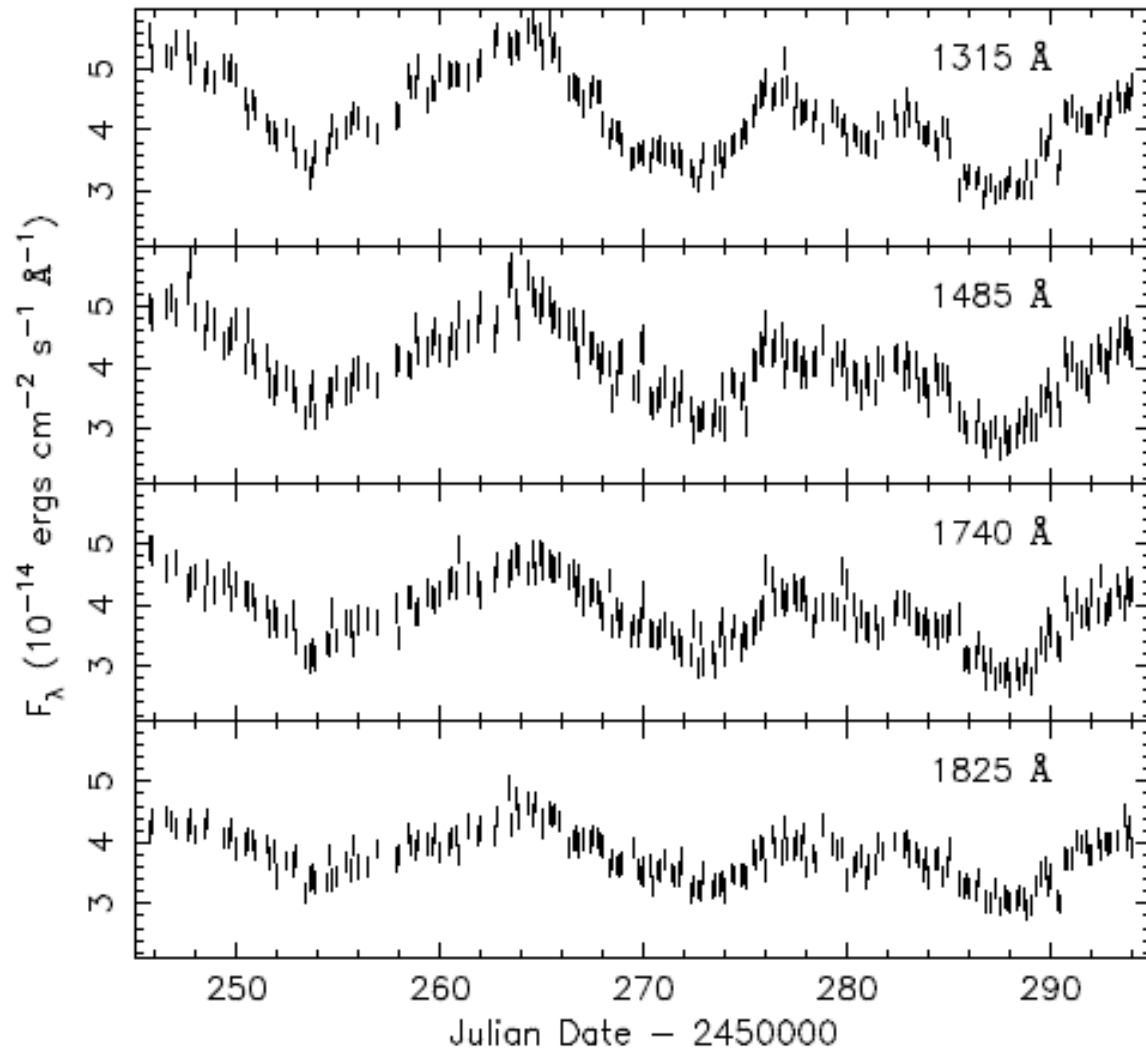
Constraints from Continuum Variability



(Crenshaw et al. 1996, ApJ, 470, 322)

- IUE* Monitoring of NGC 4151 (and other campaigns):
- UV continuum gets “bluer” as it gets brighter
 - smallest time scale ~ 2 days
 - both consistent with thin accretion disk predictions
 - no lag detected between bands:
 - 1) disturbance faster than sound speed
 - 2) UV is reprocessed radiation from X-ray corona? (irradiated disk)

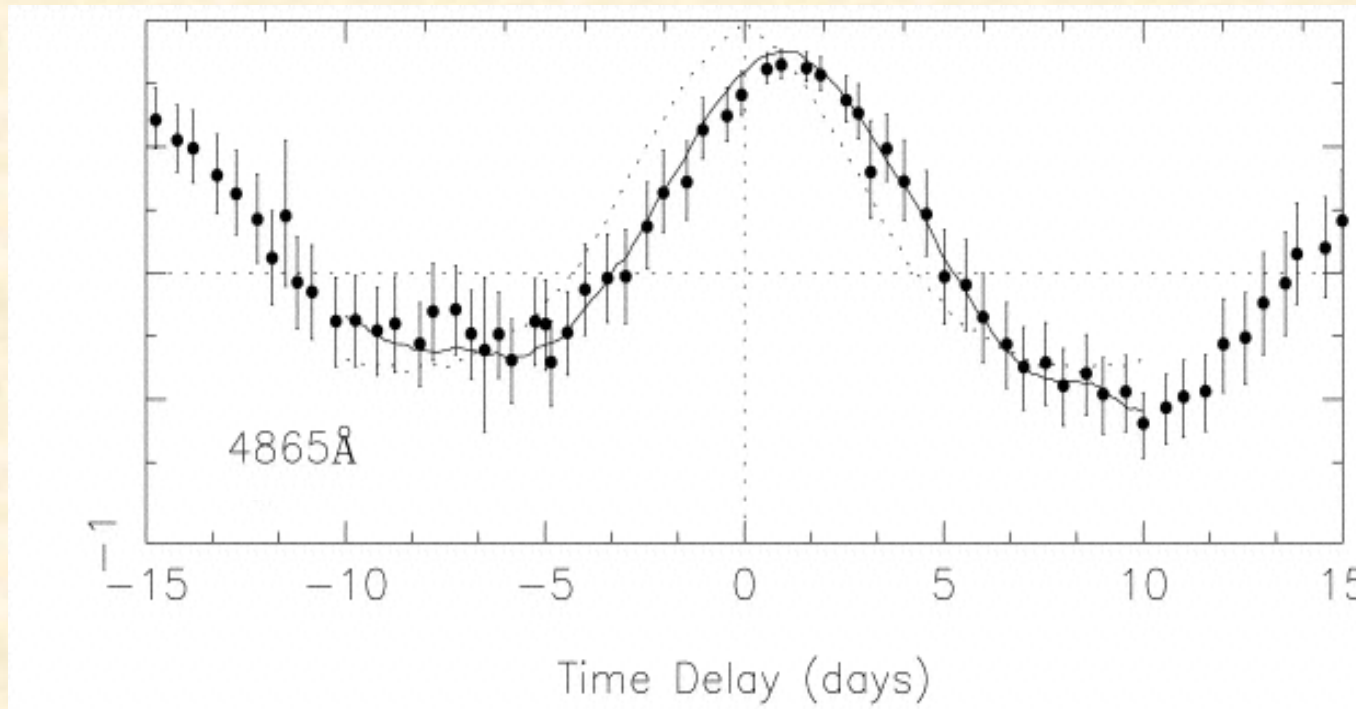
UV Continuum Variability of NGC 7469



(Wanders, et al., ApJS, 113, 69)

- most intensive IUE monitoring campaign

NGC 7469: Cross-Correlation of Optical (4865Å) with UV (1315Å)

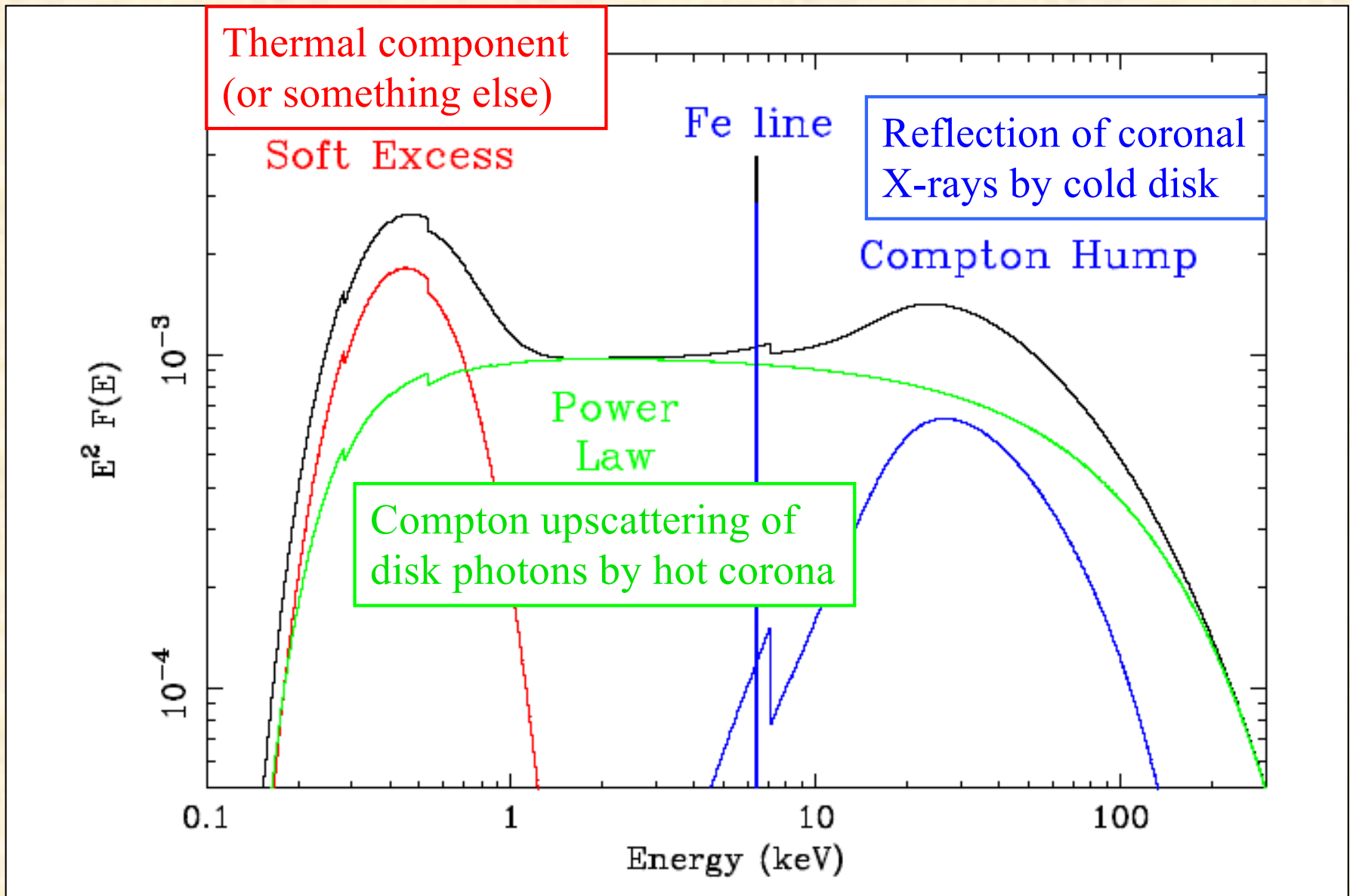


Dotted - ACF
Solid - CCF
Points - DCF
(similar to CCF)

(Colliers, et al. 1998, ApJ, 500, 162)

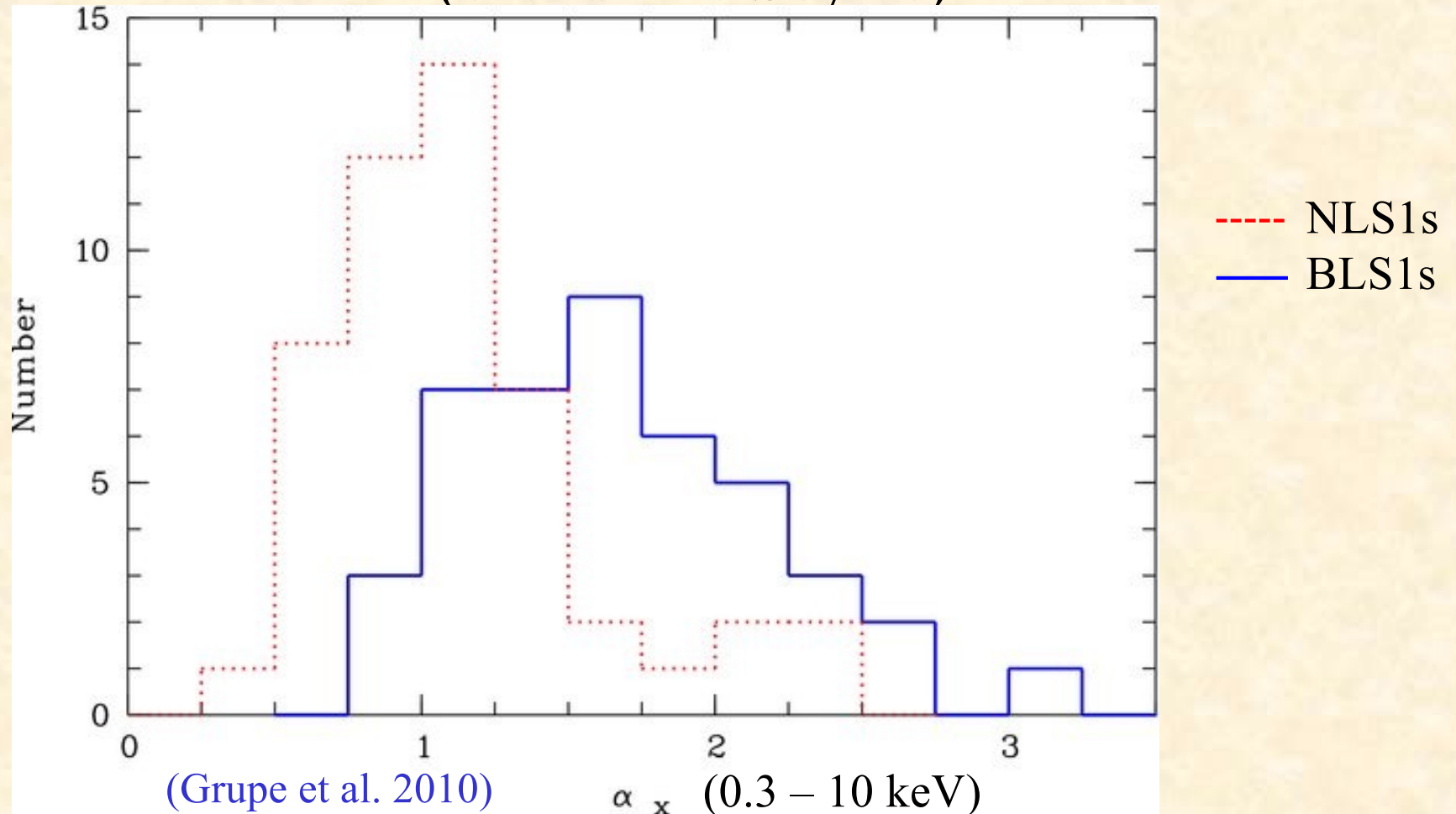
- Optical continuum lags the UV by ~ 1.2 days
- From various bins: $\text{Lag} \sim \lambda^{4/3}$
- If the lag is interpreted as a radius - results are consistent with disturbance traveling close to speed of light, not sound).
- Recent monitoring indicates accretion disks are ~ 3 times larger than predicted by thin (Shakura-Sunyaev) disk (Fausnagh+ 2018, ApJ, 854, 107)

2) X-ray Emission: Components



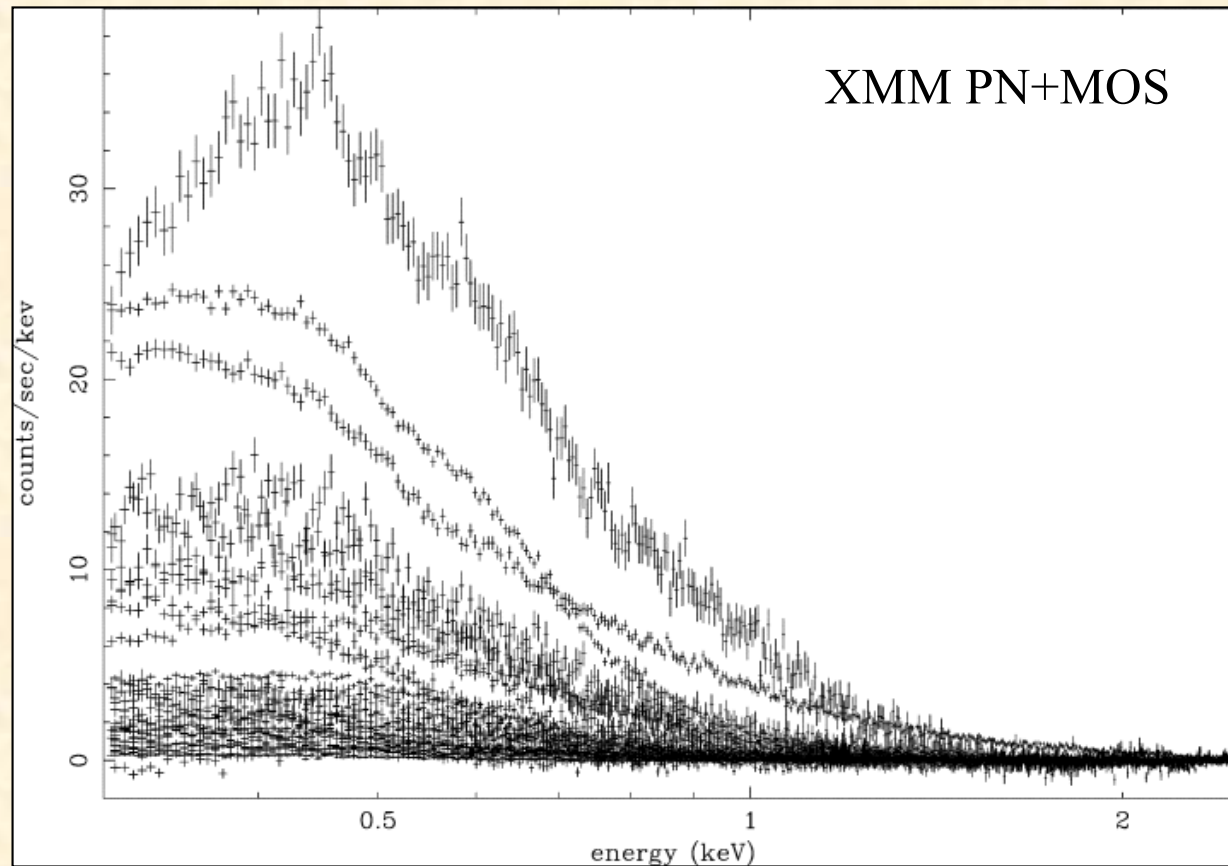
(Fabian, 2006, AN, 327, 943)

Power Laws: NLS1s compared to BLS1s (broad-line Sey 1s)



- NLS1s show steeper slopes than BLS1s in both soft (0.2 – 2 keV) and hard (2 – 10 keV) X-ray bands
- NLS1s show more rapid X-ray variability than BLS1s (Boller et al. 1996; Brandt et al. 1997)

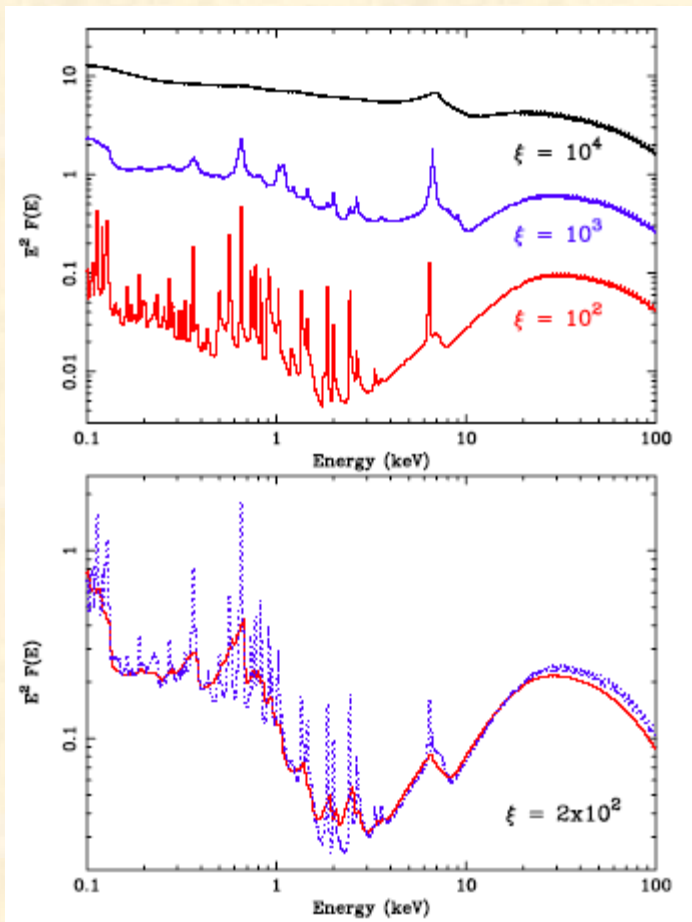
Soft X-ray Excess



(Crummy, et al. 2006, MNRAS, 365, 1067)

- Seyfert 1s and quasars show a soft X-ray excess below 1 keV after subtraction of power-law (NLS1s show more soft X-ray excess)
- Previously explained by a thermal component (e.g., low-temperature Comptonization of accretion disk photons).

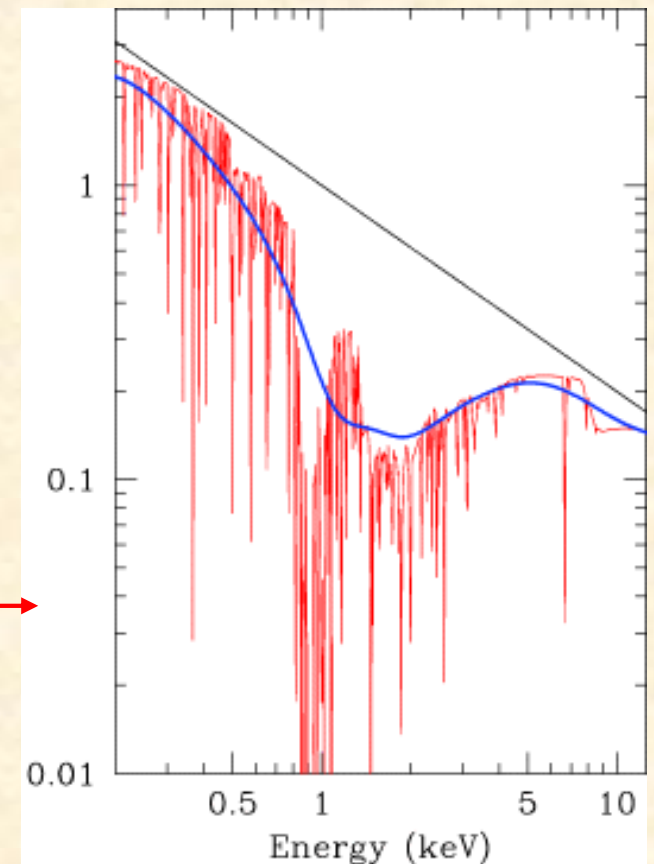
- But the excess has a fixed “temperature” (~ 0.2 keV), suggesting an atomic rather than continuum origin (Done & Nayakshin, 2007, MNRAS, 377, L59):
 - 1) Relativistically broadened (“blurred”) emission lines from accretion-disk **reflection** (Crummy, et al. 2006).
 - 2) High-velocity outflows of ionized gas **absorbing** the 0.7 - 3 keV range (Done & Nayakshin, 2007; Chevallier, et al. 2006, A&A, 449, 493).



(Fabian, 2006, AN, 327, 943)

← 1) Reflection

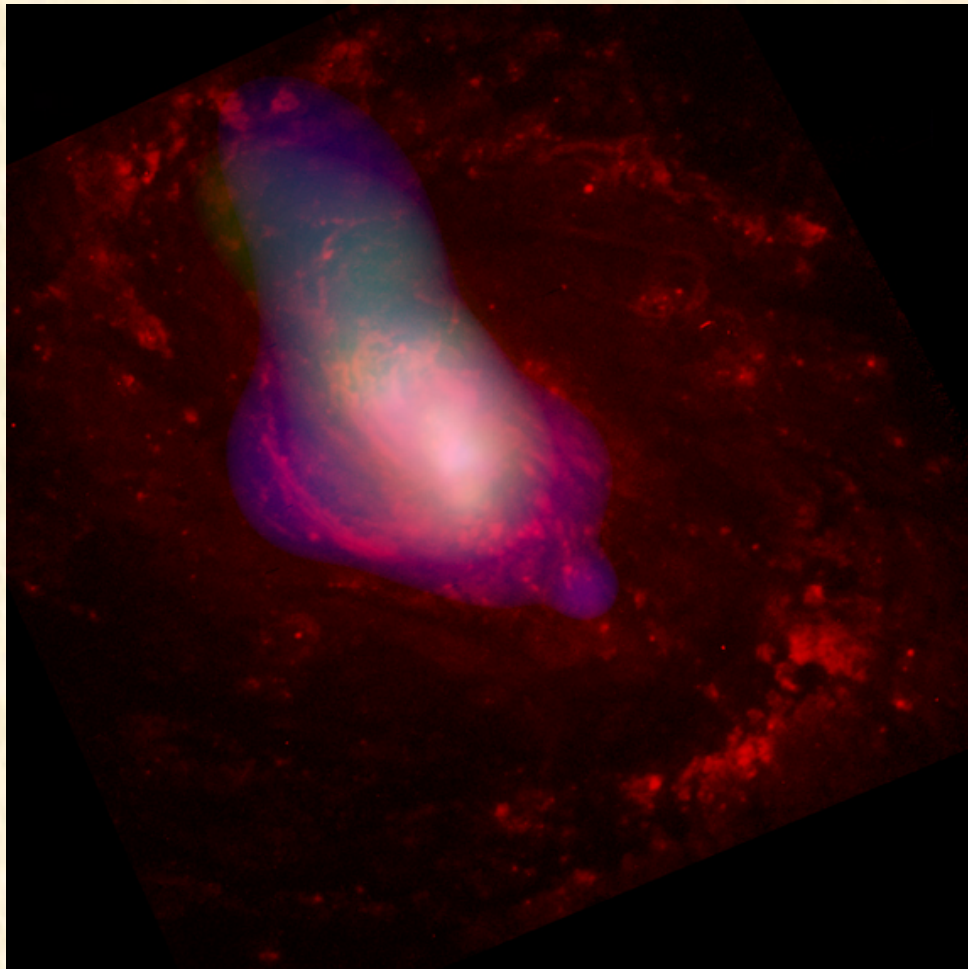
2) Absorption →



(Gierlinski & Done, 2004, MNRAS, 349, L7)

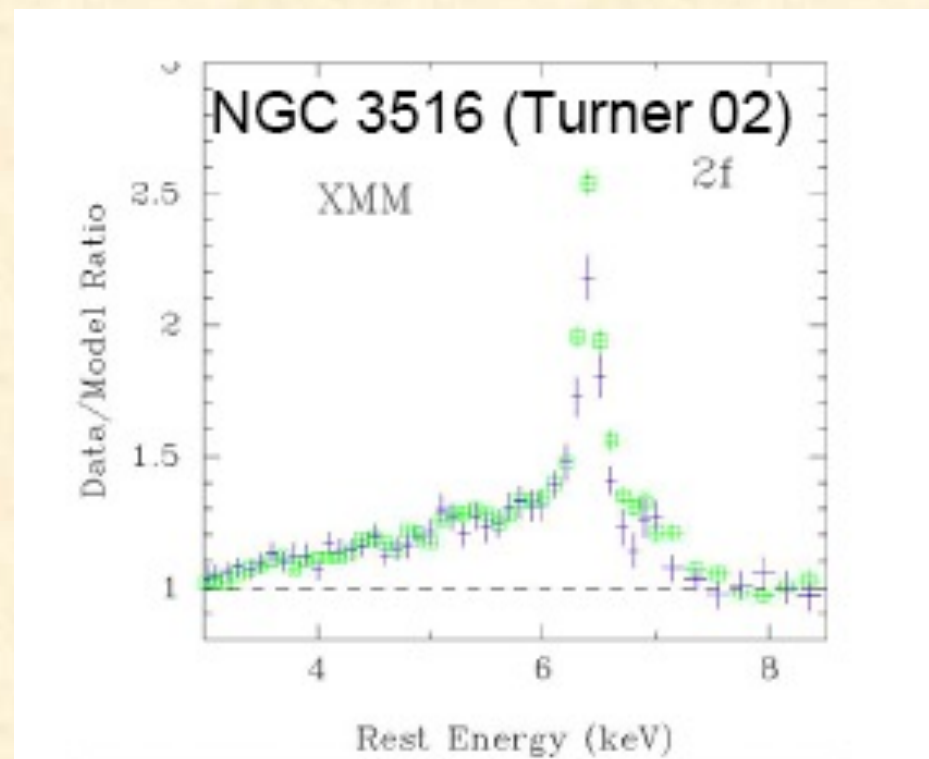
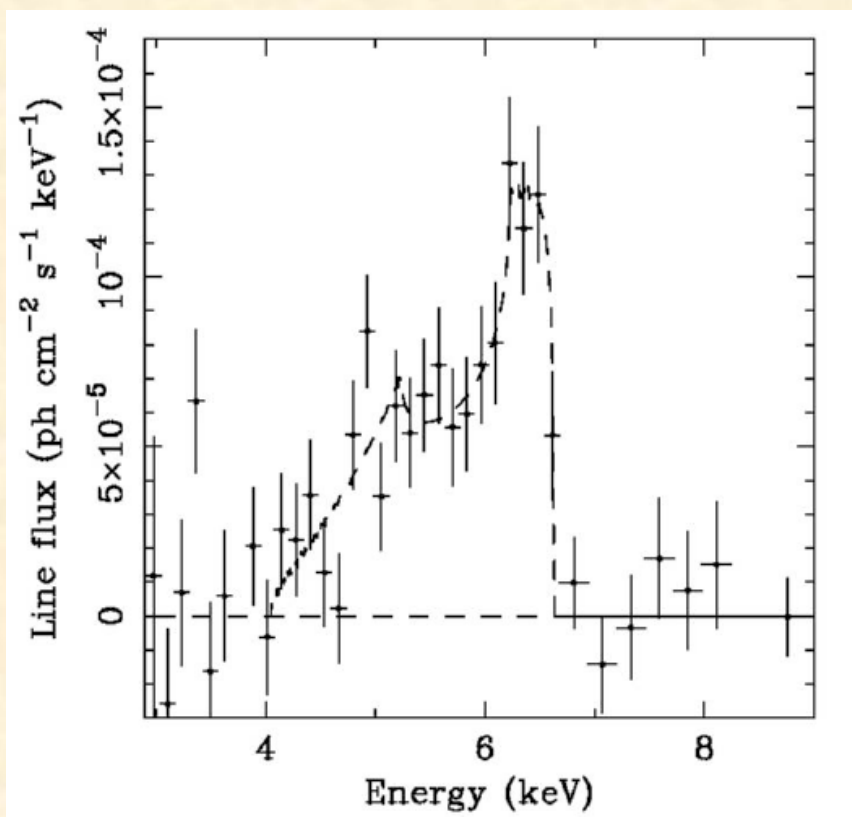
- In nearby Seyferts with obscured (NGC 1068) or temporarily faint (NGC 4151) central engines, the majority of the soft X-ray emission comes from an **extended region roughly coincident with the NLR**:

CXO/HST Image of NGC 1068



(Ogle, et al. 2003, A&A, 849, 864)

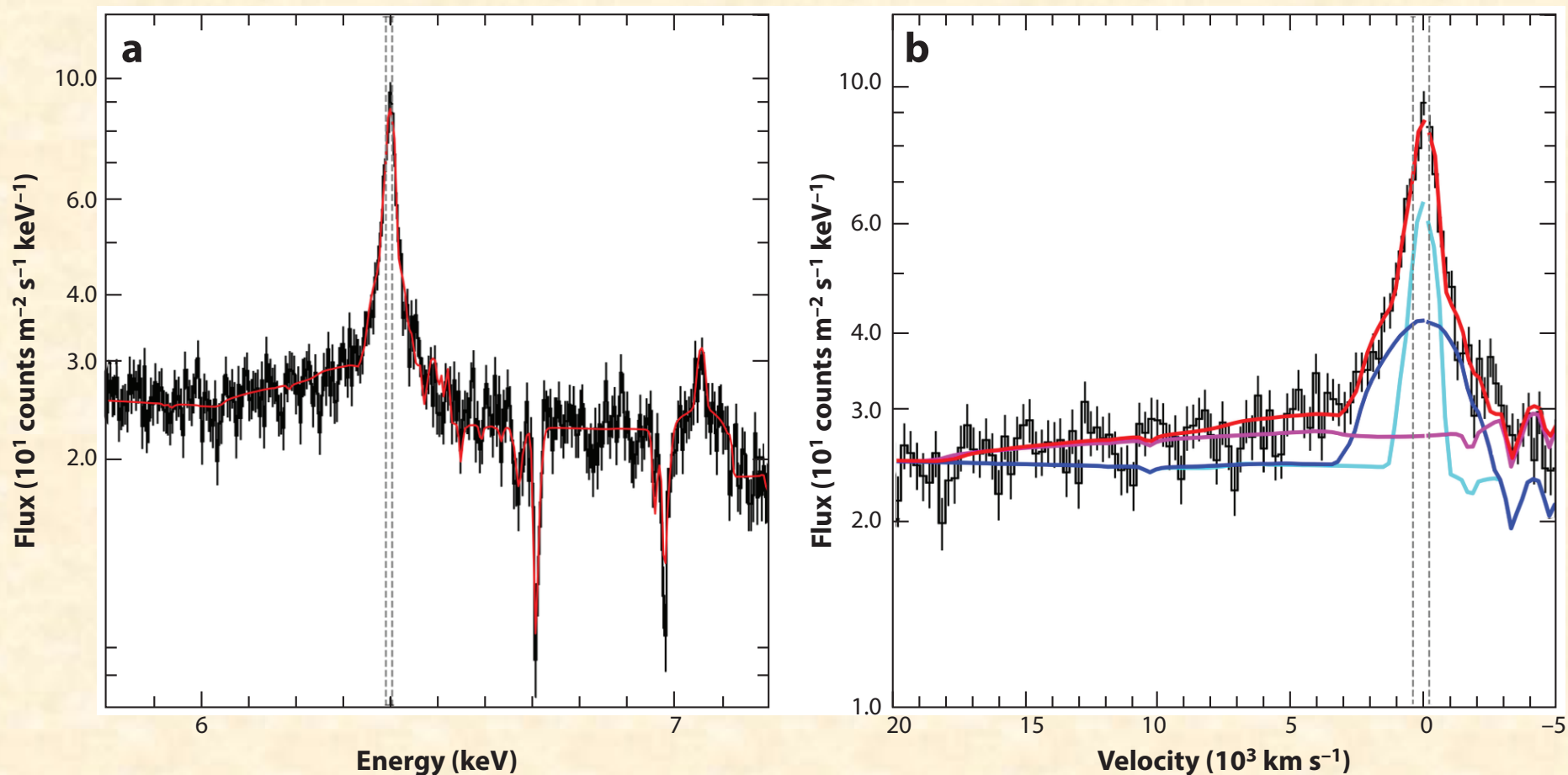
Fe K α Emission Lines



MCG -6-30-15 (Tanaka et al. 1995)

- ASCA detected a number of broad Fe K α emission lines in Seyfert 1s
- Gravitationally redshifted wing - direct evidence for accretion disk origin
- From ionization of K-shell electron and subsequent $n=2 \rightarrow 1$ transition
- Chandra and XMM observations find most Fe-K α lines show strong “narrow” components - could be from BLR, inner NLR, or torus
- Broad Fe K-alpha confirmed with Suzaku, NuStar observations

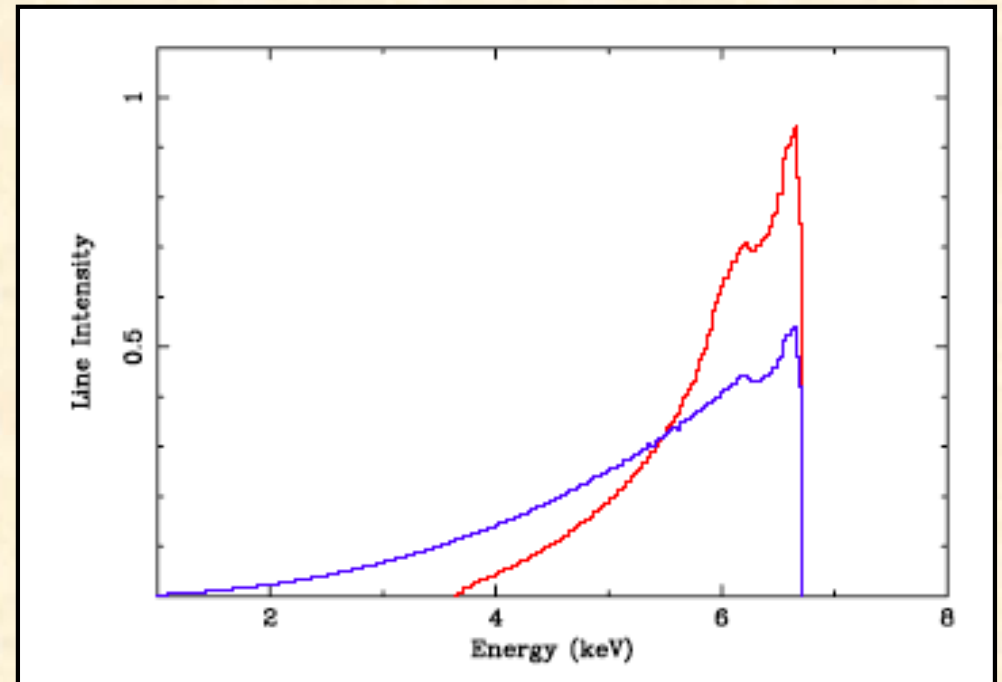
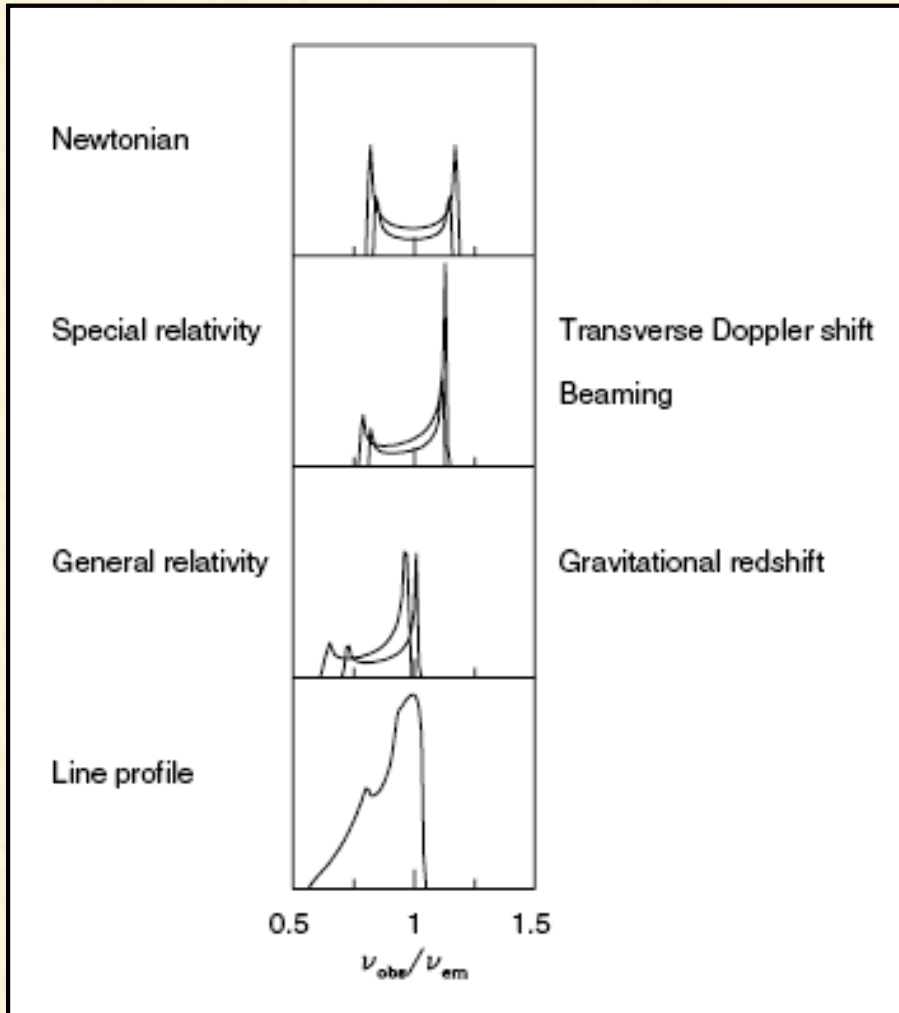
XRISM Observations of NGC 4151



(Audard+ 2024, ApJ, 923, L25)

- XRISM microcalorimeter ($R \sim 1200$) can easily resolve the “narrow” component of Fe $K\alpha$.
- Reflection from torus (cyan), BLR (blue), and outer accretion disk (red).
- Need large energy range to get the “broad” component (inner accretion disk).

Broad Fe K α - Accretion Disk Models



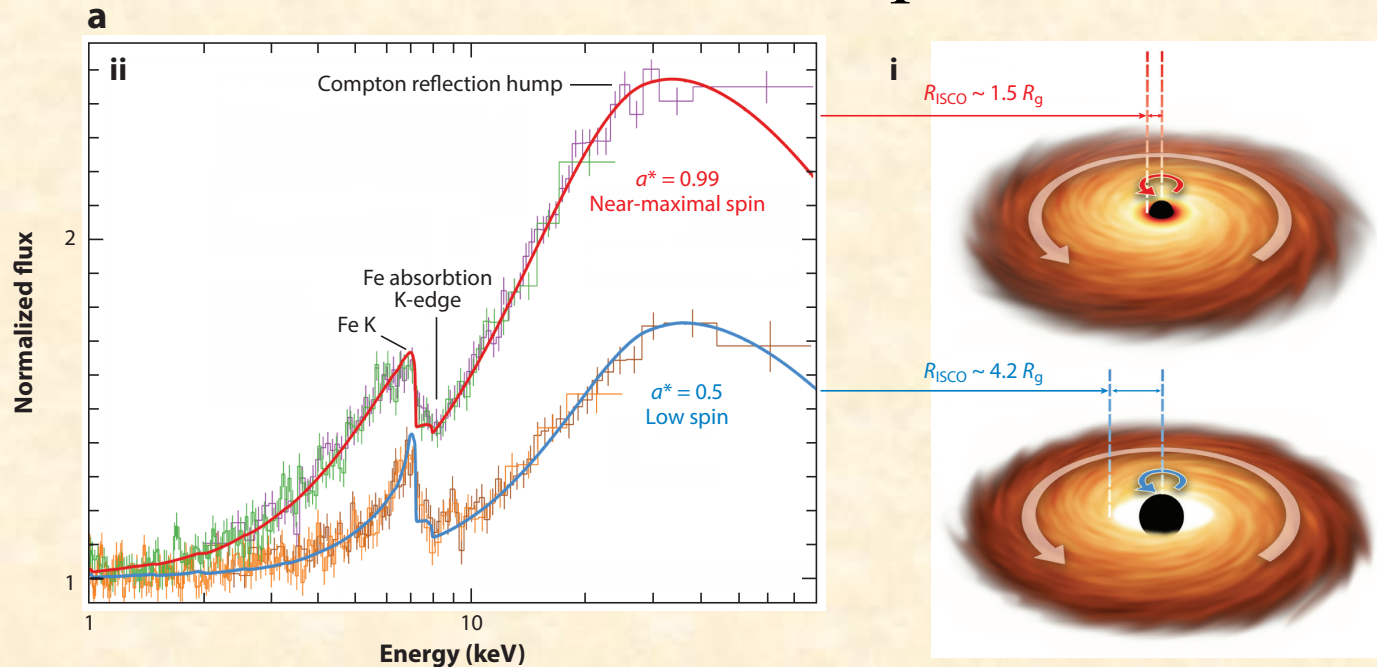
(Fabian, 2006, AN, 327, 943)

--- Schwarzschild BH, inner radius = $6 r_g$

--- Kerr BH, inner radius = $1.24 r_g$

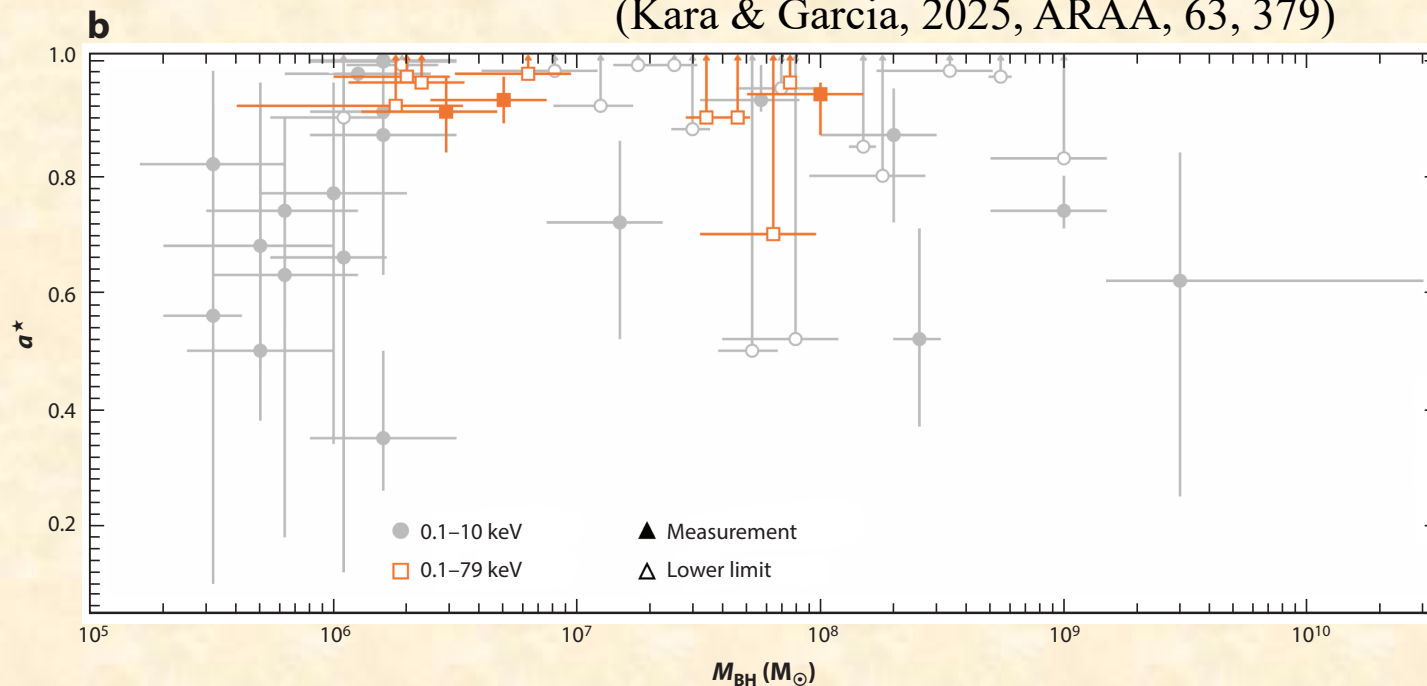
Ultimate goal: fit profile to get the black hole spin (a) and accretion disk inclination

SMBH Spin Results



- Simulated XMM-Newton / NuSTAR spectrum and fit

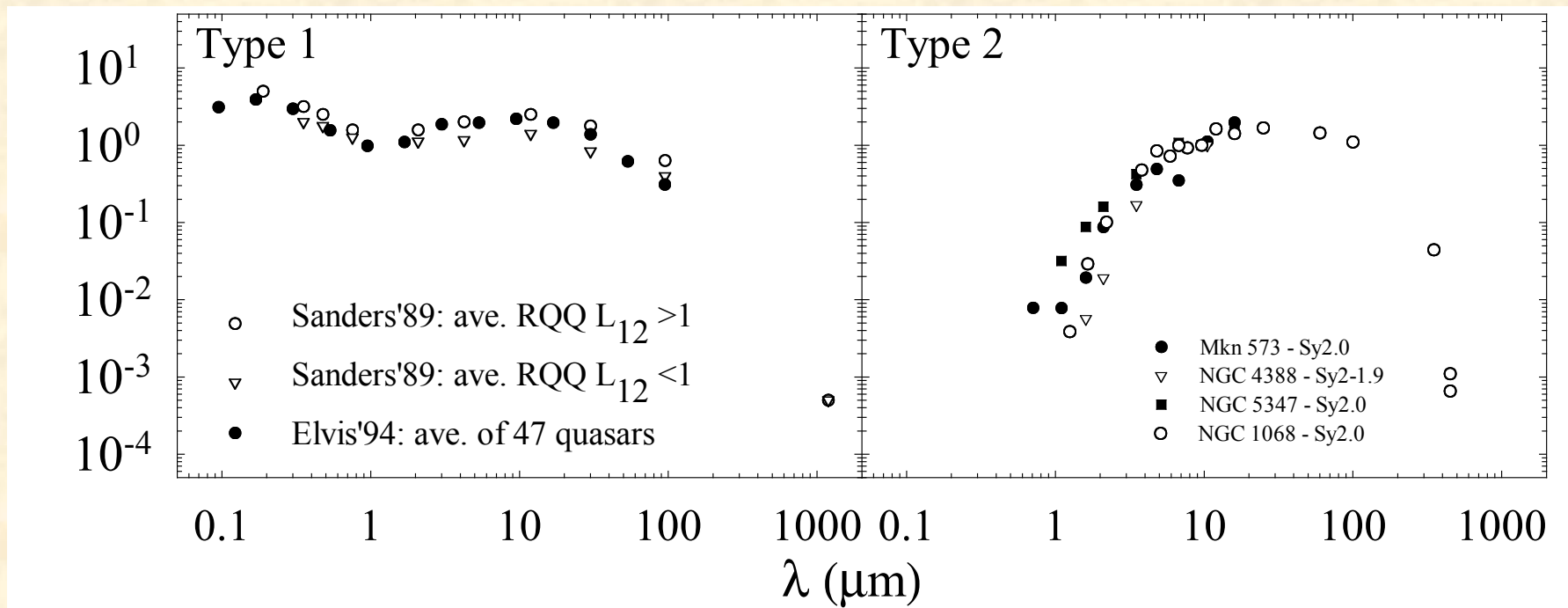
(Kara & Garcia, 2025, ARAA, 63, 379)



- Note movement to high spin values when constrained by full energy range

- Need XRISM and high-energy (e.g., NuSTAR) to fully constrain spins (in progress).

3) IR Bump and the “Torus”

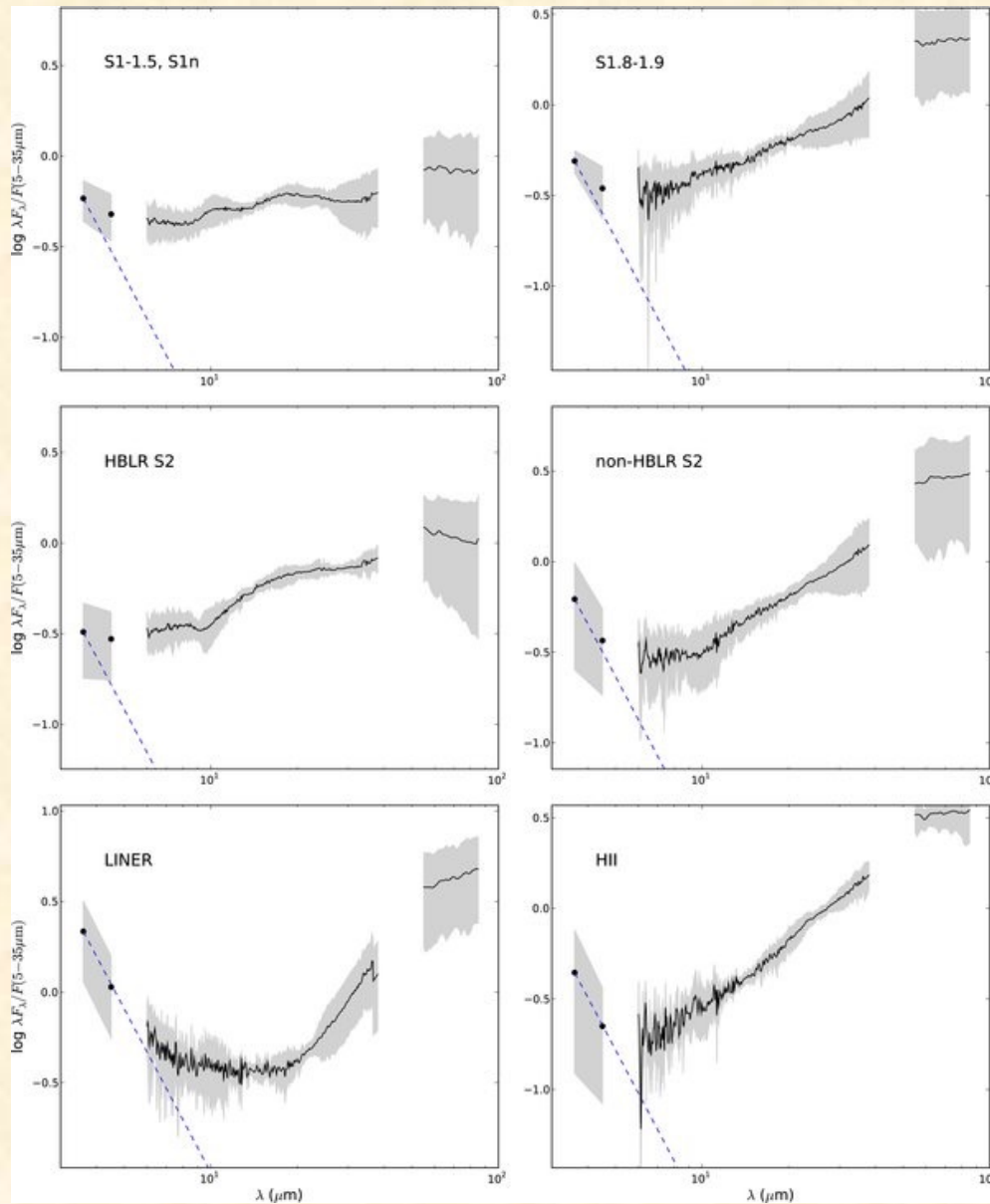


Prior to Spitzer:

- Seyfert 1s show strong optical/UV from accretion disk
- Both Seyfert 1s and 2s show strong mid-IR emission indicating hot dust near AGN (and colder dust from star formation regions)
- Dip at $1 \mu\text{m}$ in Sey 1s because dust sublimates at $\sim 1500 \text{ K}$
- Inner edge of torus given by dust sublimations radius:

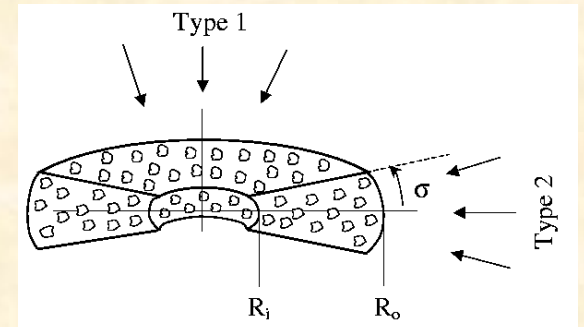
$$r = 1.3L_{46}^{1/2}T_{1500}^{-2.8} \approx 0.1 \text{ pc for Seyferts (Barvainis 1987)}$$

Spitzer Observations (20'' apertures)



- Sey 1s and Sey 2s with hidden BLRs are dominated by hot dust in mid-IR
- Other types dominated by star formation: colder dust and PAH emission features
- Sey 1s tend to show **weak** silicate emission at $10 \mu\text{m}$
- Sey 2s show **weak** silicate absorption
- If smooth tori, weakness of silicate absorption is not consistent with large X-ray columns ($N_{\text{H}} = 10^{23} - 10^{24} \text{cm}^{-2}$) in many Sey 2s, suggesting the torus is *clumpy*.

Clumpy Emission - Anisotropy



(Nenkova 2002, ApJ, 570, L9)

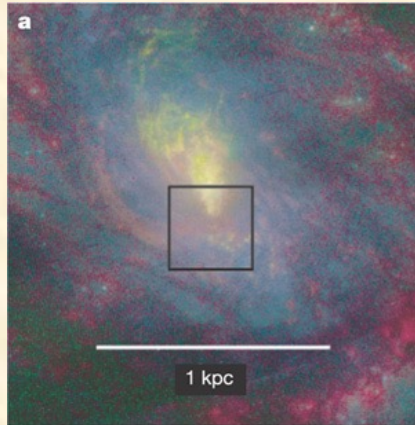


(from M. Elitzur)

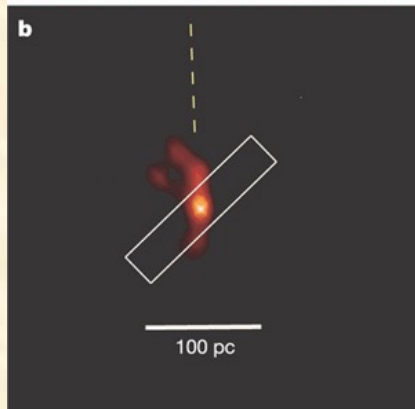
- X-ray column is large if clump(s) cover the central source in the line of sight.
- Silicate $10 \mu\text{m}$ absorption in Sey 2s is filled in by view of irradiated faces.
- Silicate emission in Sey 1s is weakened by absorption in some clumps.
- IR SEDs are more uniform, because you see unobstructed emission at any angle.

Resolving the Torus: Mid-IR Interferometry of NGC 1068

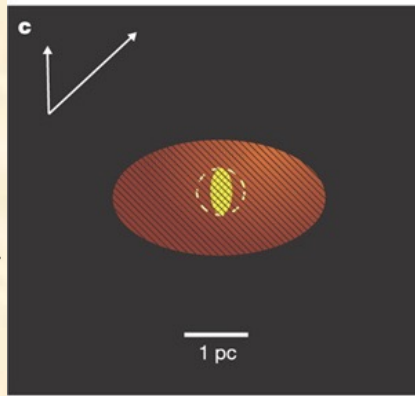
HST
optical



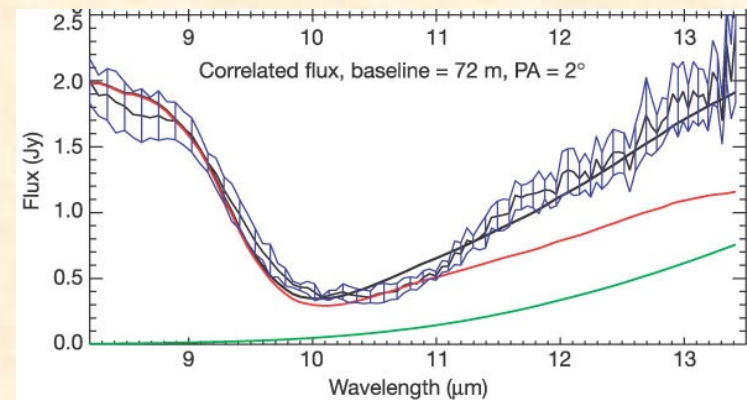
VLT
8.7 μm
image



VLTI
Interfer.

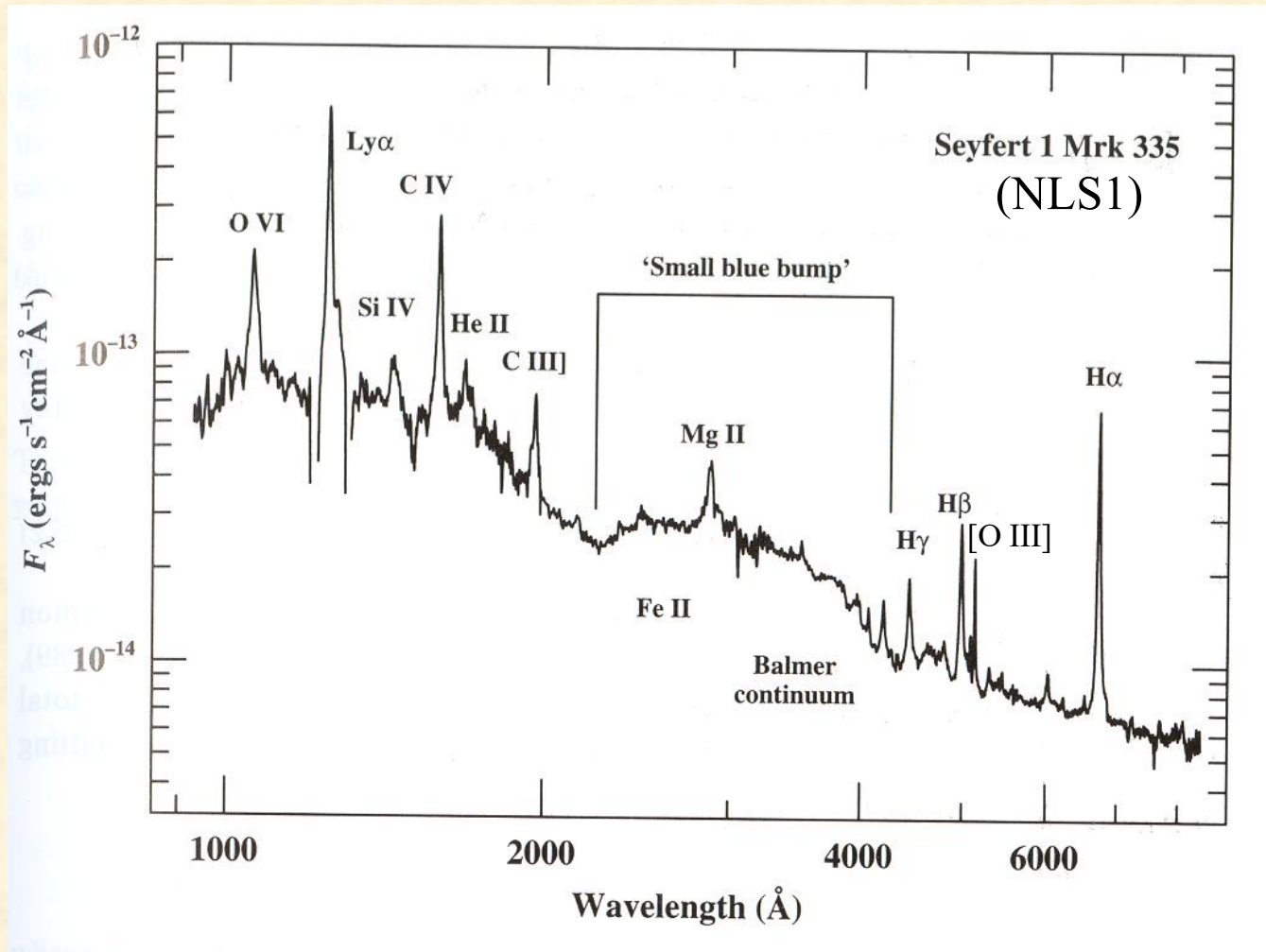


- Extended N-S structure due to hot dust in NLR
- VLTI Interferometry + spectroscopy at $\sim 10\mu\text{m}$
- Warm (320 K) dust from 2.1×3.4 pc structure
- Hot (> 800 K) from marginally resolved structure (~ 10 mas ≈ 0.7 pc)
- Silicate $10\mu\text{m}$ absorption from edge-on view



(Jaffe, et al. 2004, Nature, 429, 47)

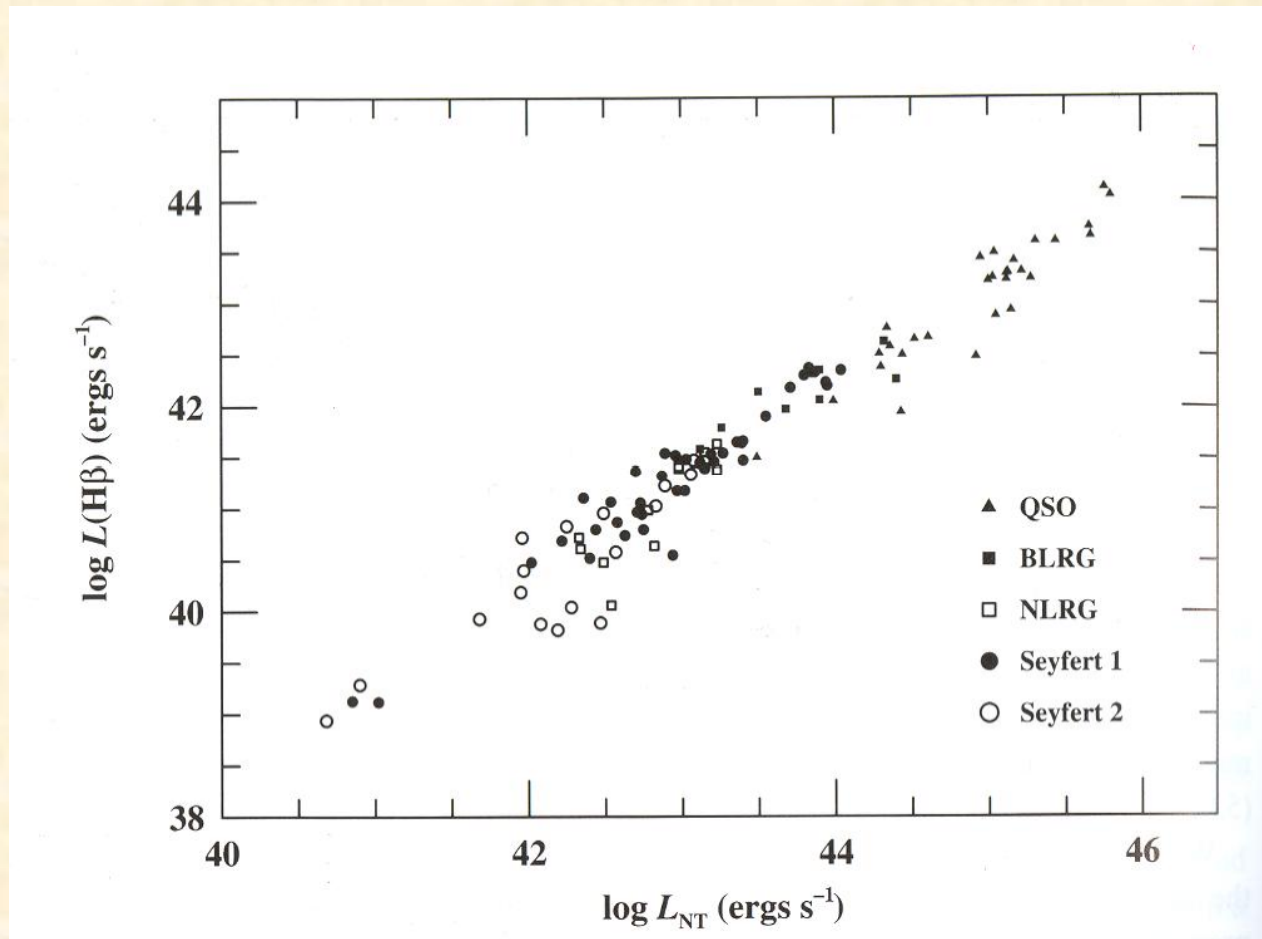
4) Broad Emission Lines



(Peterson, p. 71)

- Mrk 335: FWHM ([O III]) $\approx 500 \text{ km s}^{-1}$, FWHM (C III]) $\approx 2000 \text{ km s}^{-1}$
- no broad [O III], broad C III], strong Fe II $\rightarrow n_{\text{H}} = 10^9 - 10^{11} \text{ cm}^{-3}$

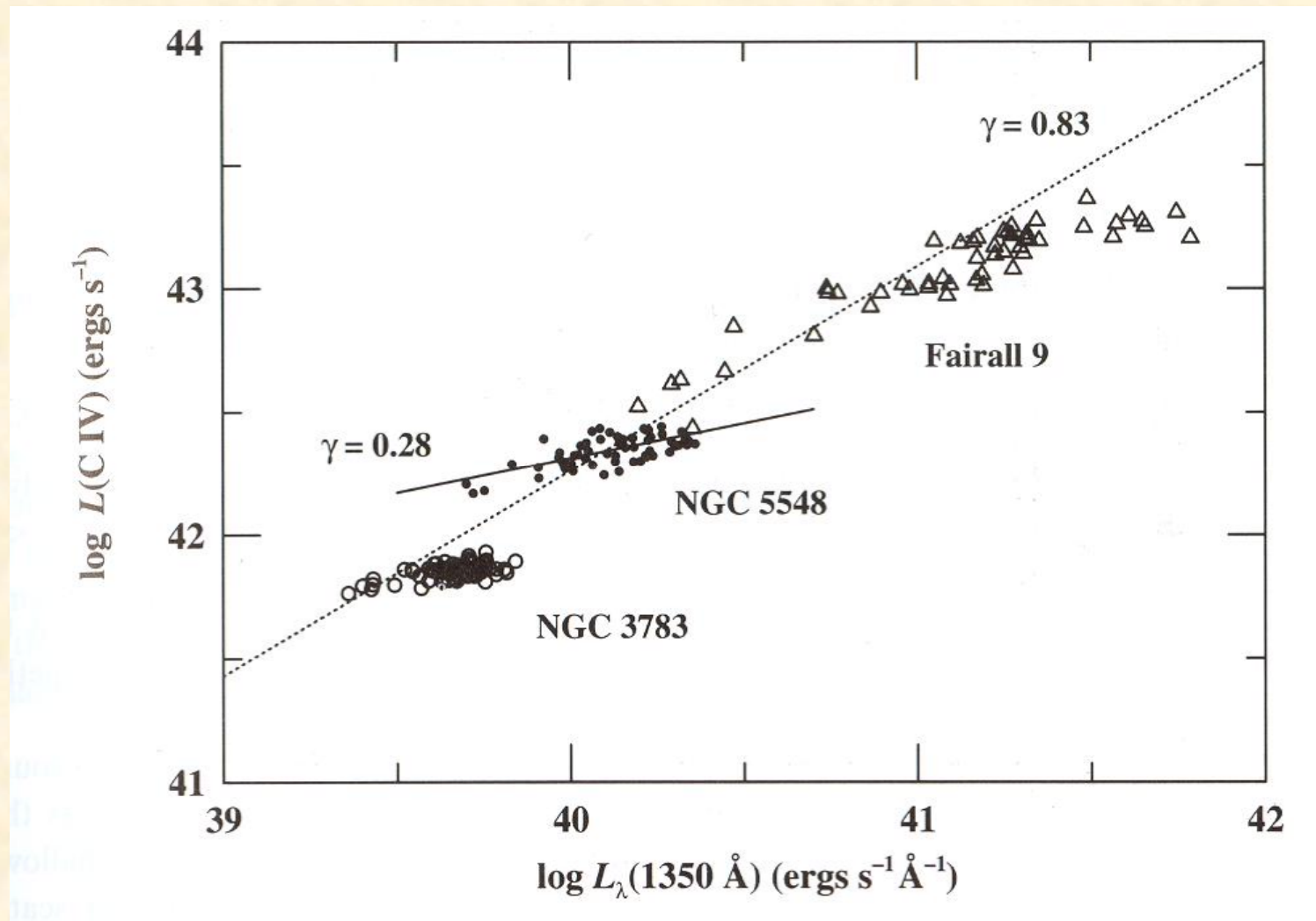
Emission Lines vs. Nonthermal Continuum



(Peterson, p. 90)

- Emission-line and continuum luminosities correlated over broad range
→ Both BLR and NLR are photoionized
- Temperatures $\sim 10,000 - 20,000$ K (shocks predict much higher temps.)

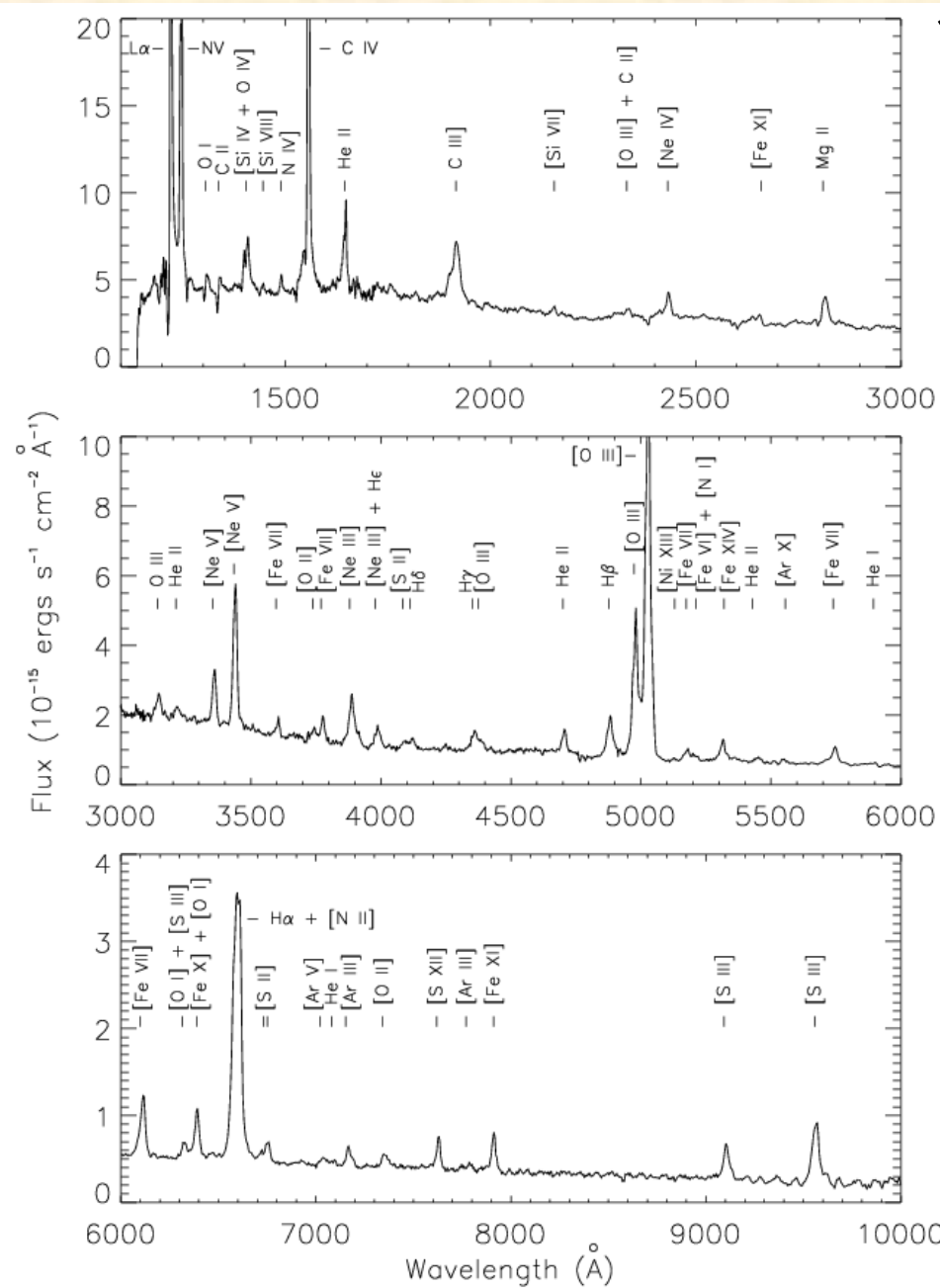
The “Baldwin Effect”



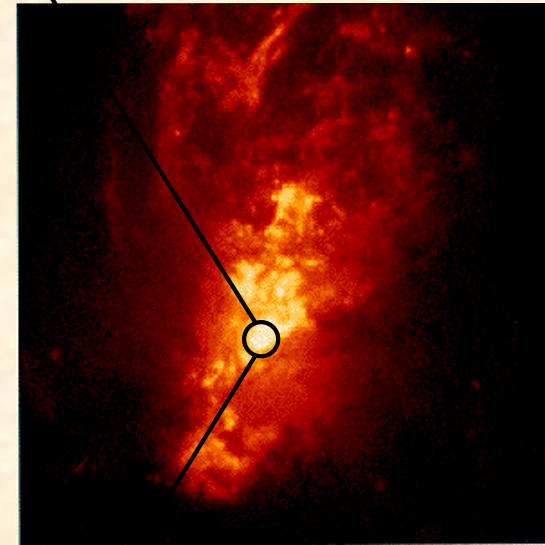
(Peterson, p. 91)

- EW (C IV) decreases with increasing luminosity for a large sample of AGN
- Same relation for individual (variable) AGN, but flatter slope
- Could be due to change in ionizing continuum and/or covering factor of BLR

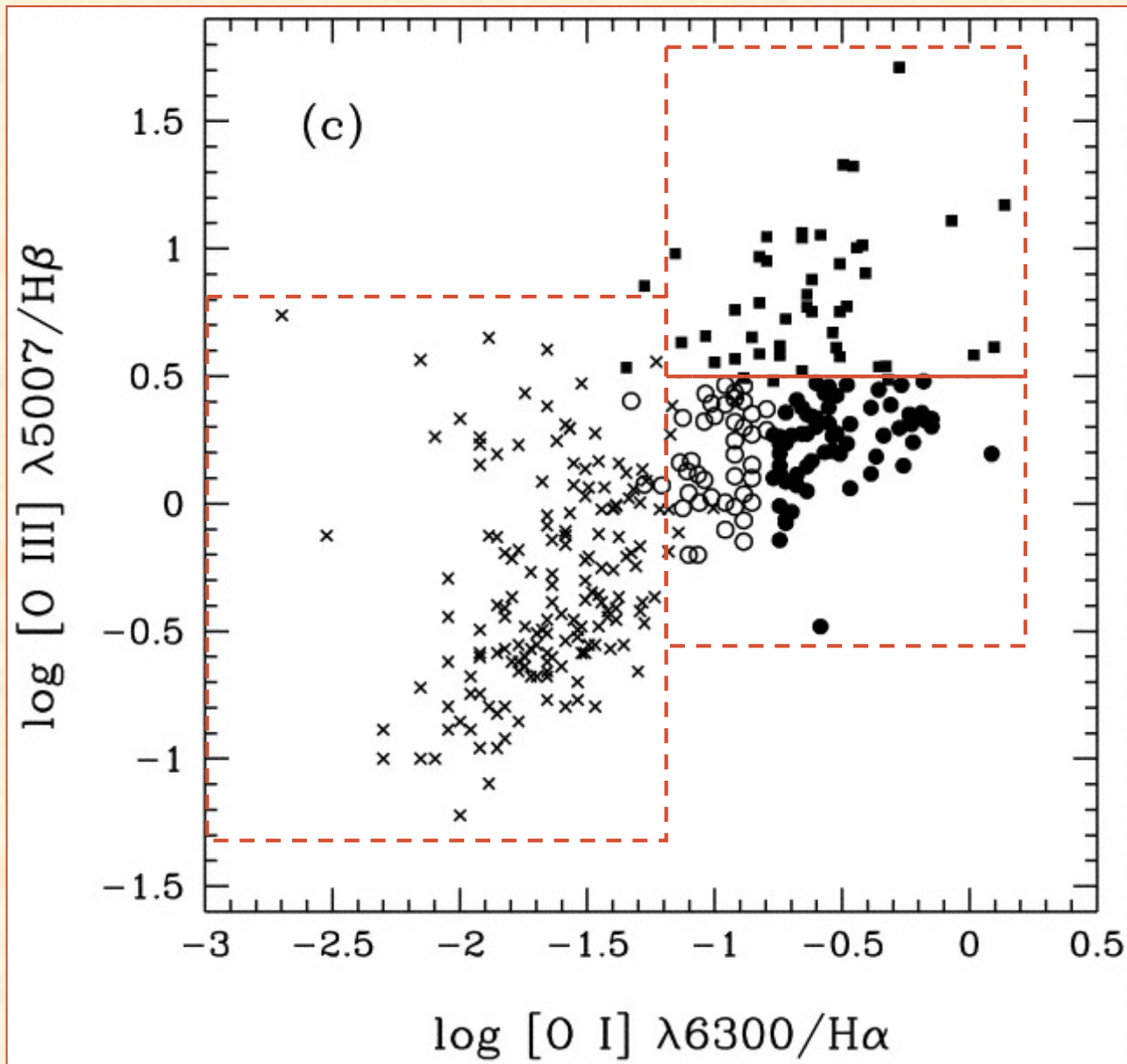
5) Narrow Line Region



HST/STIS spectrum of NGC 1068 (Seyfert 2)



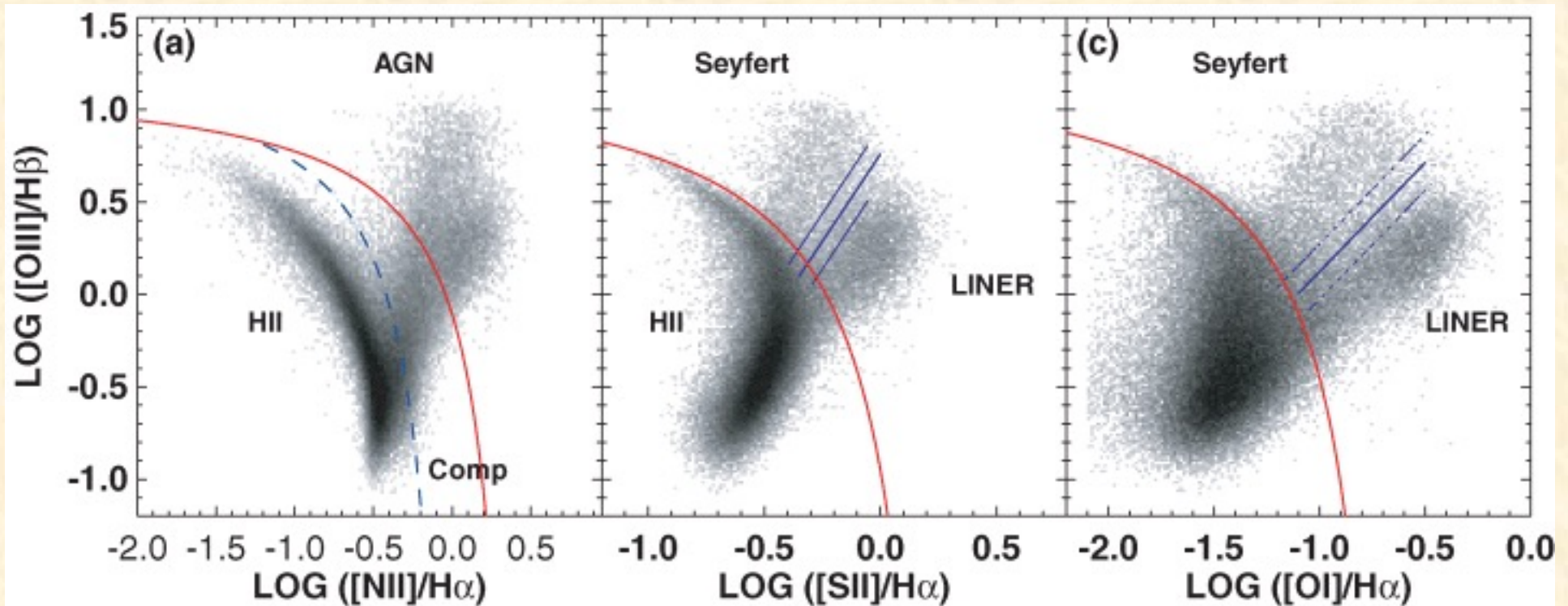
Emission-Line Diagnostics (BPT Diagram)



- x - H II galaxy
- - Seyfert NLR
- - “pure” LINER
- - transition object (H II + LINER)

(Ho, Filippenko, & Sargent, 1997, ApJS 112, 315)

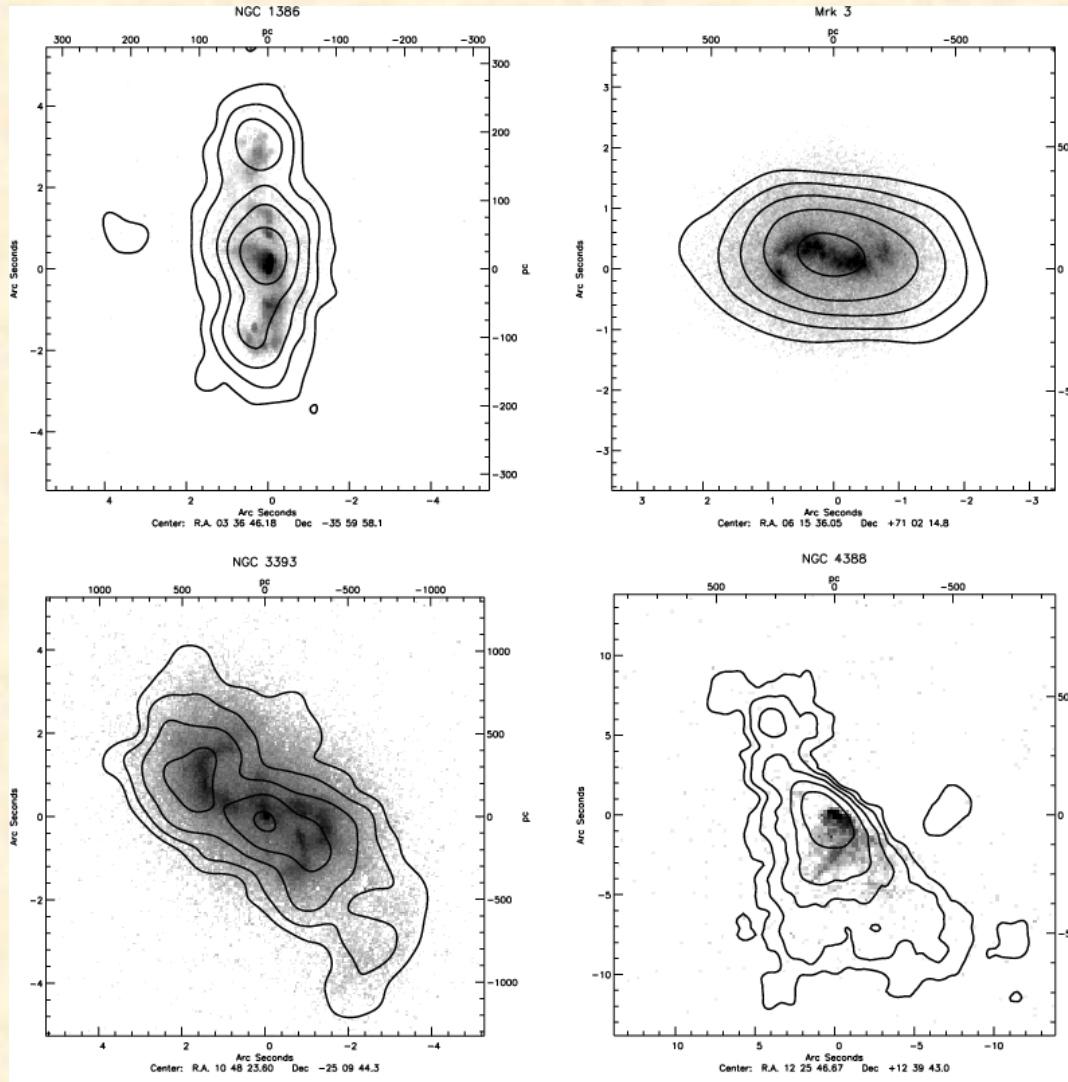
BPT Diagrams (85,000 galaxies from SDSS)



(Kewley et al. 2006, MNRAS, 372, 961)

- H II (starburst) sequence from low to high metallicity (left to right)
- Composite (“transition”) objects between blue and red lines in 1st figure
- Seyfert/LINER transition given as middle blue line in 2nd and 3rd figures (increasing ionization from lower right to upper left)

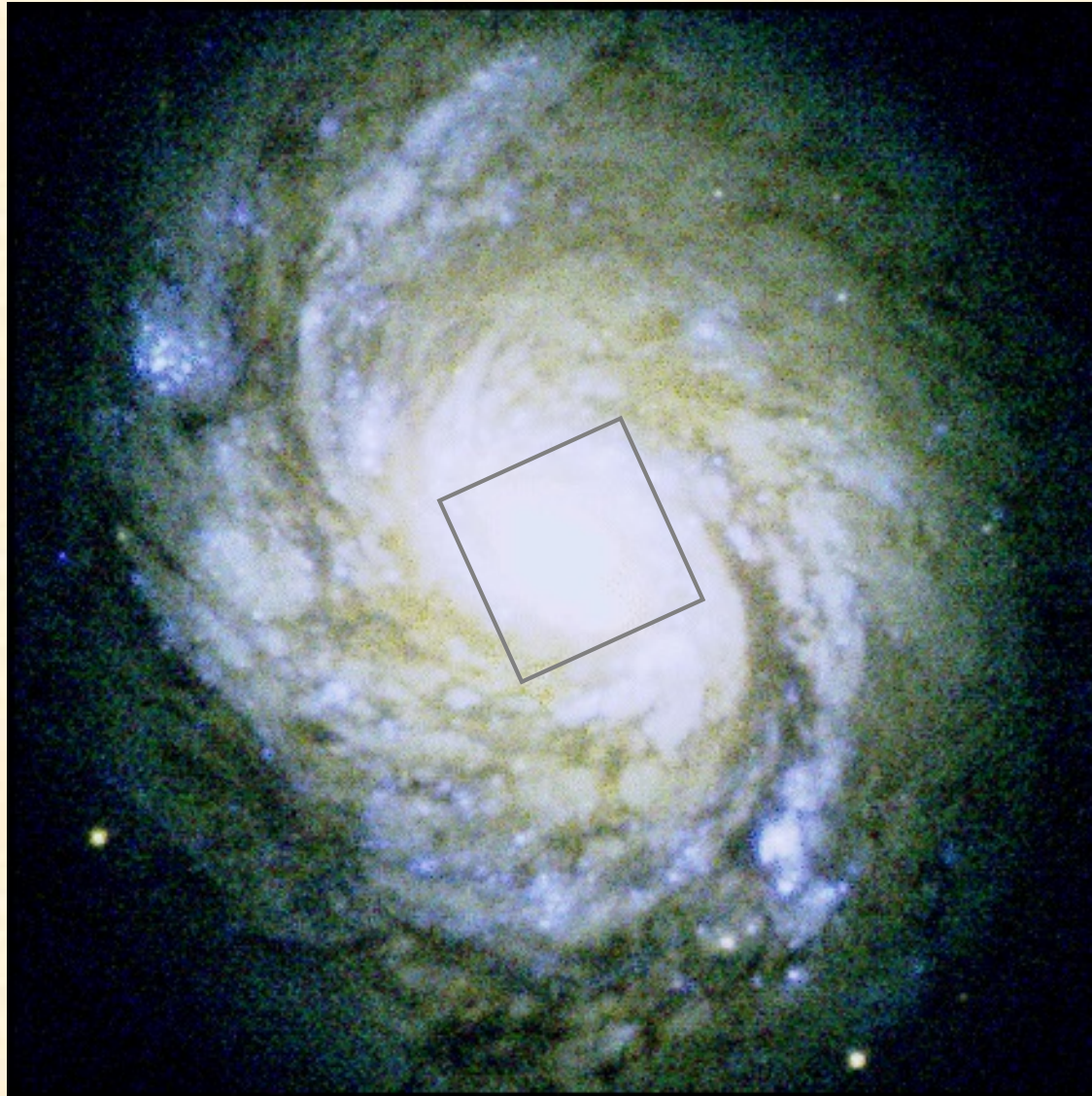
Narrow Line Region – Now Resolvable



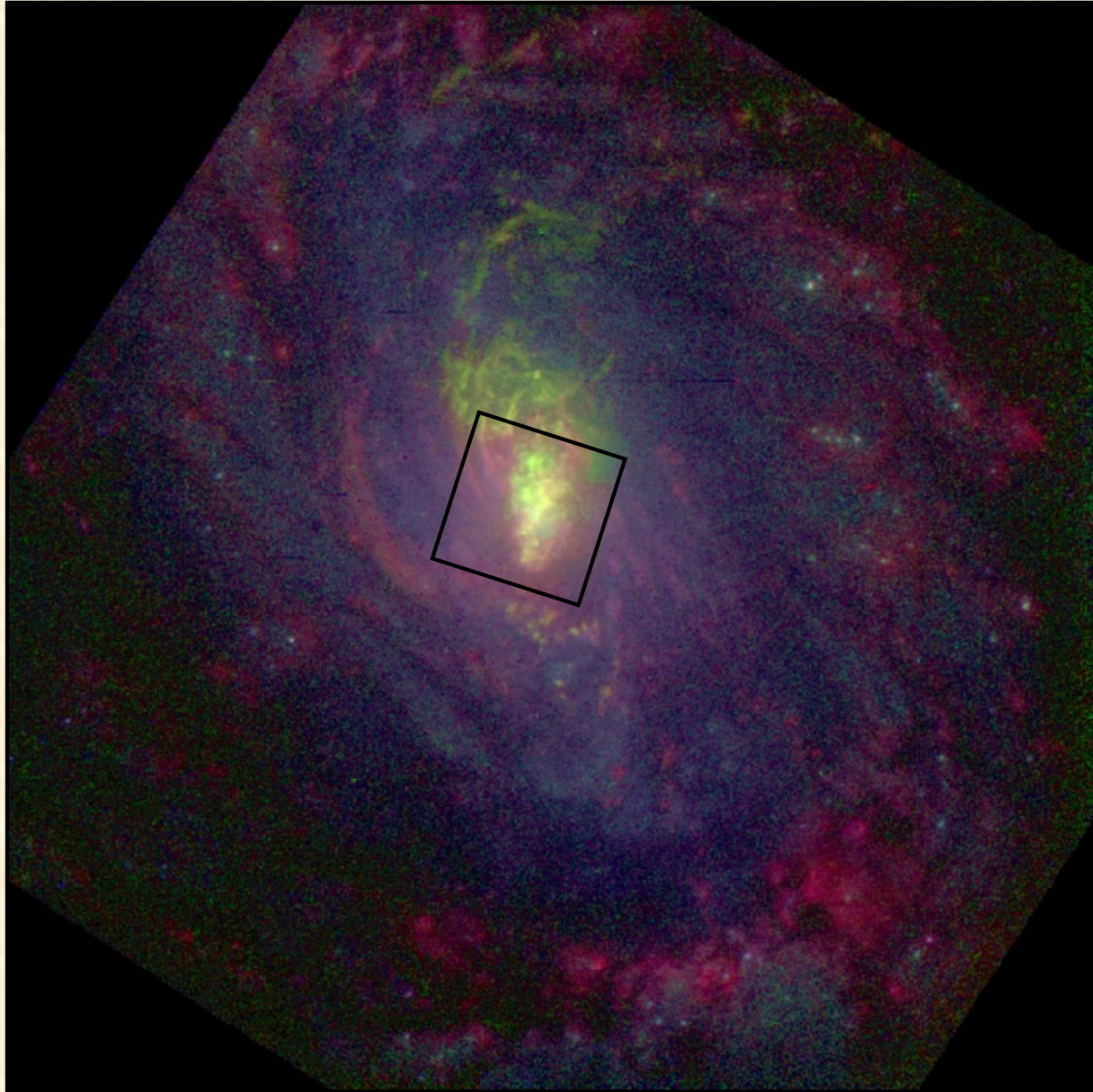
Greyscale:
HST [O III] emission
Contours:
Chandra Soft X-rays

(Bianchi et al. 2006, A&A, 448, 499)

Ex) NGC 1068: Ground-based Image
CFHT, 3' x 3' (13 x 13 kpc)



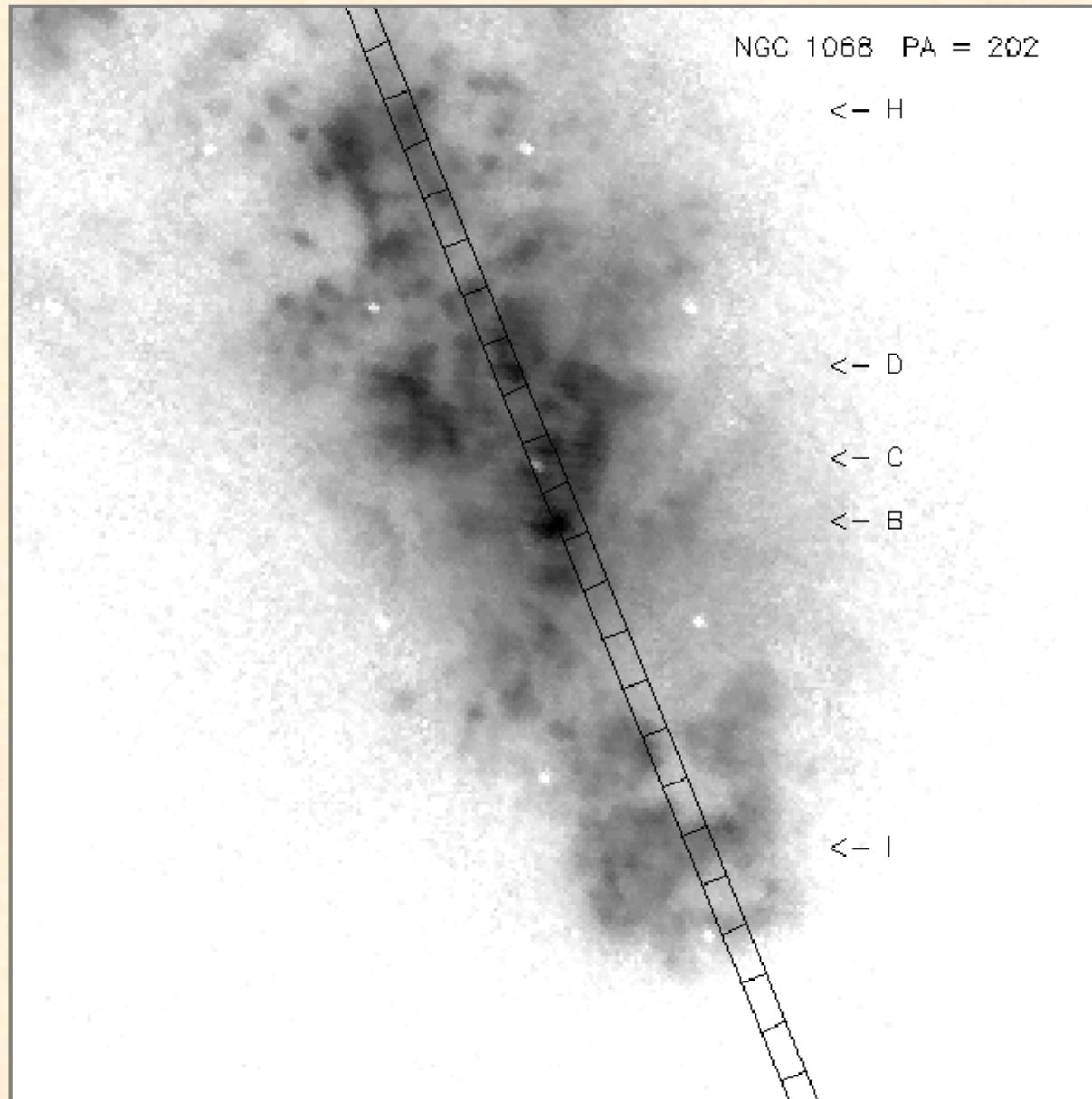
NGC 1068 – HST/WFPC2 Image
(Bruhweiler et al. 2001, ApJ, 546, 866)



blue - stellar
red - $H\alpha$
green - [O III]

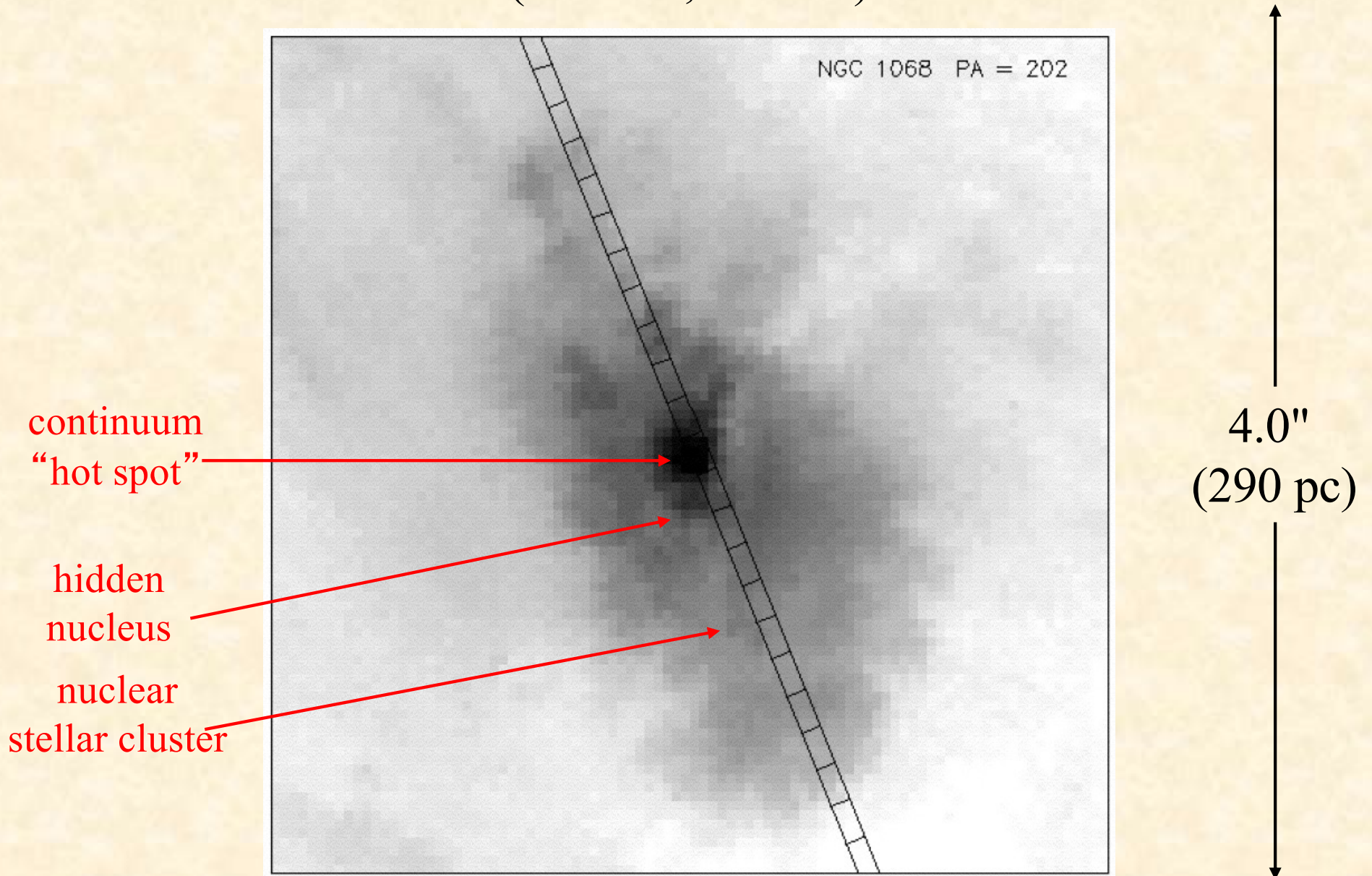
NGC 1068: NLR

STIS slit: 52" x 0.1" on FOC [O III] Image

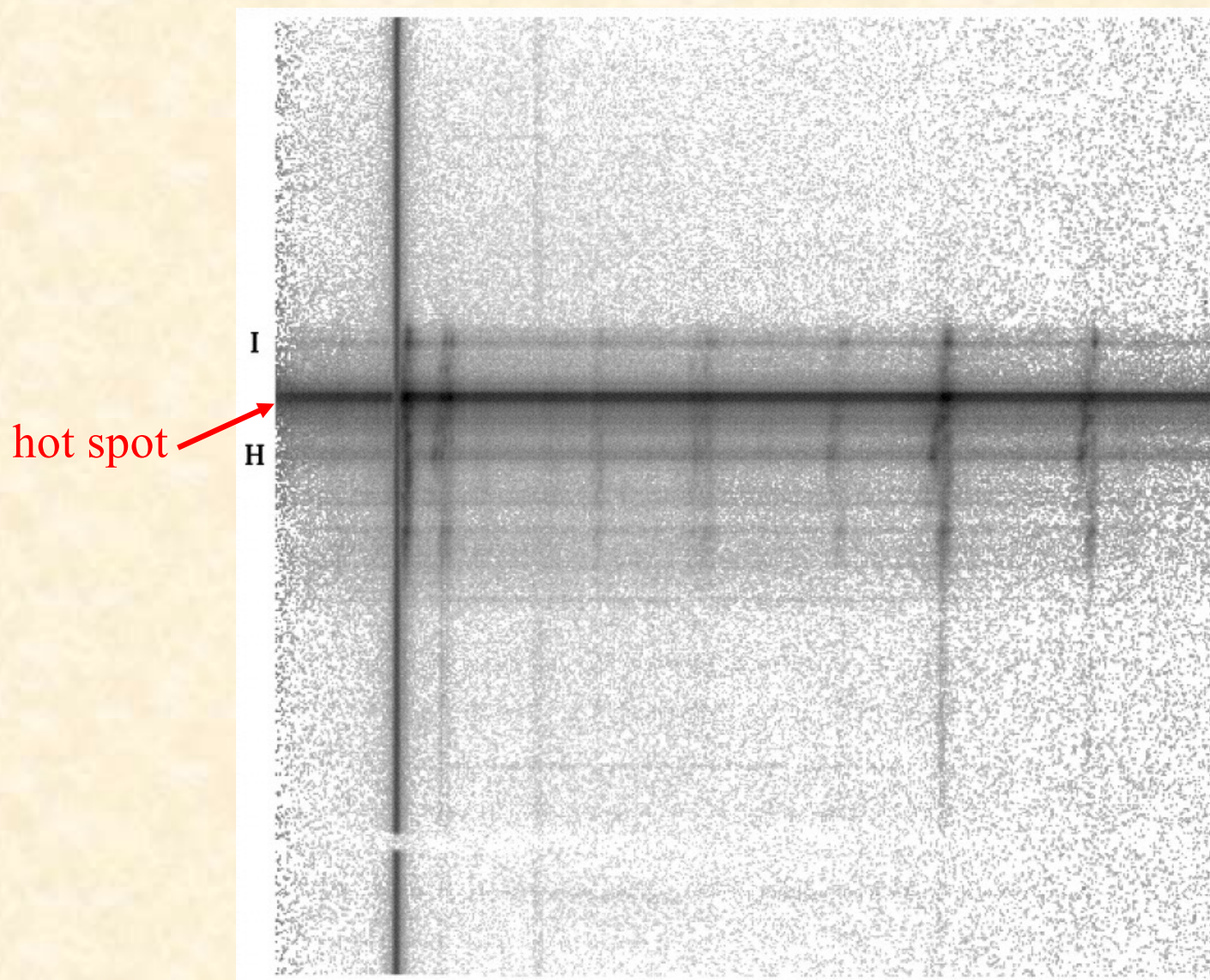


4.0"
(290 pc)

NGC 1068: Continuum Image (WFPC2, F547M)

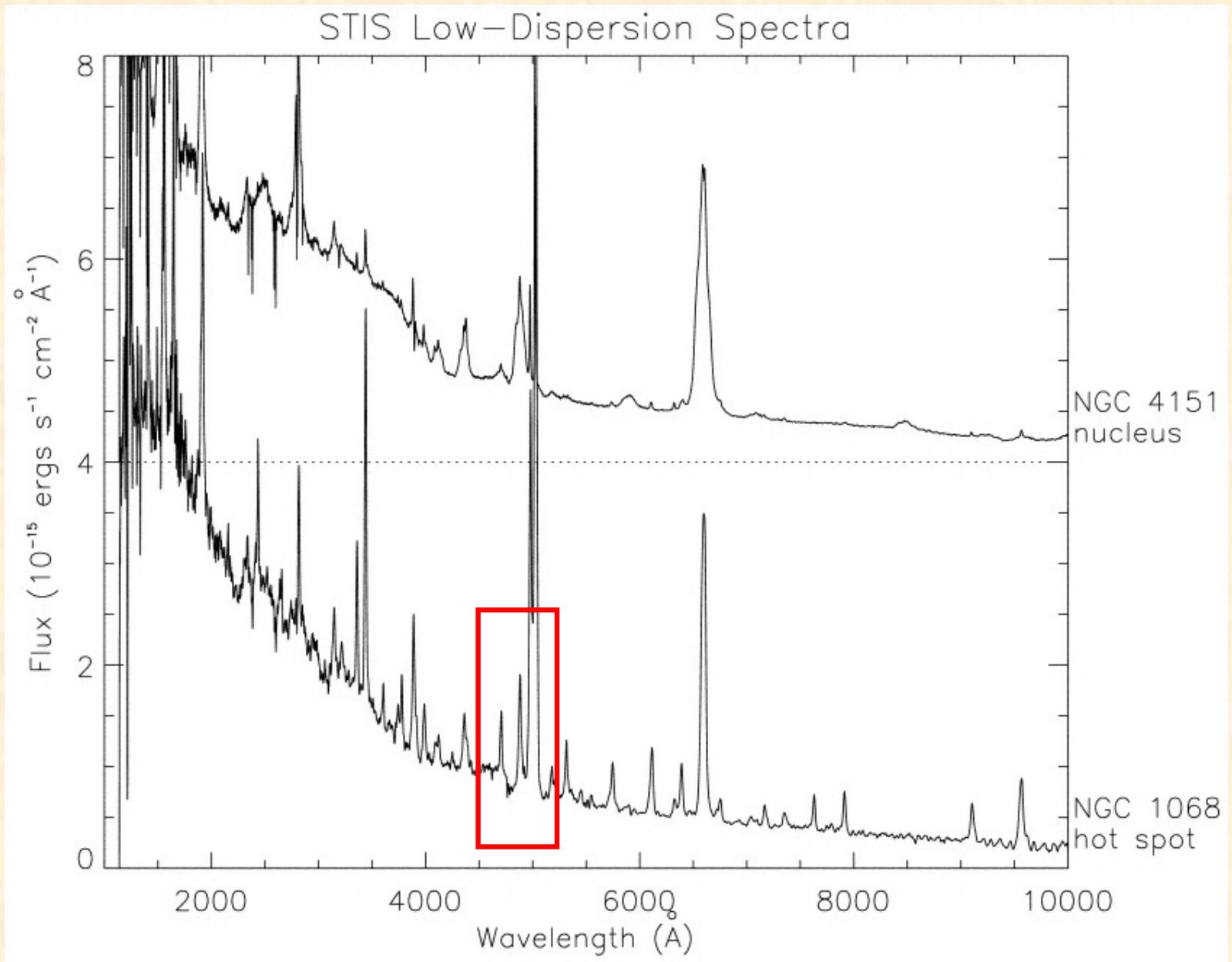


Scattered Light

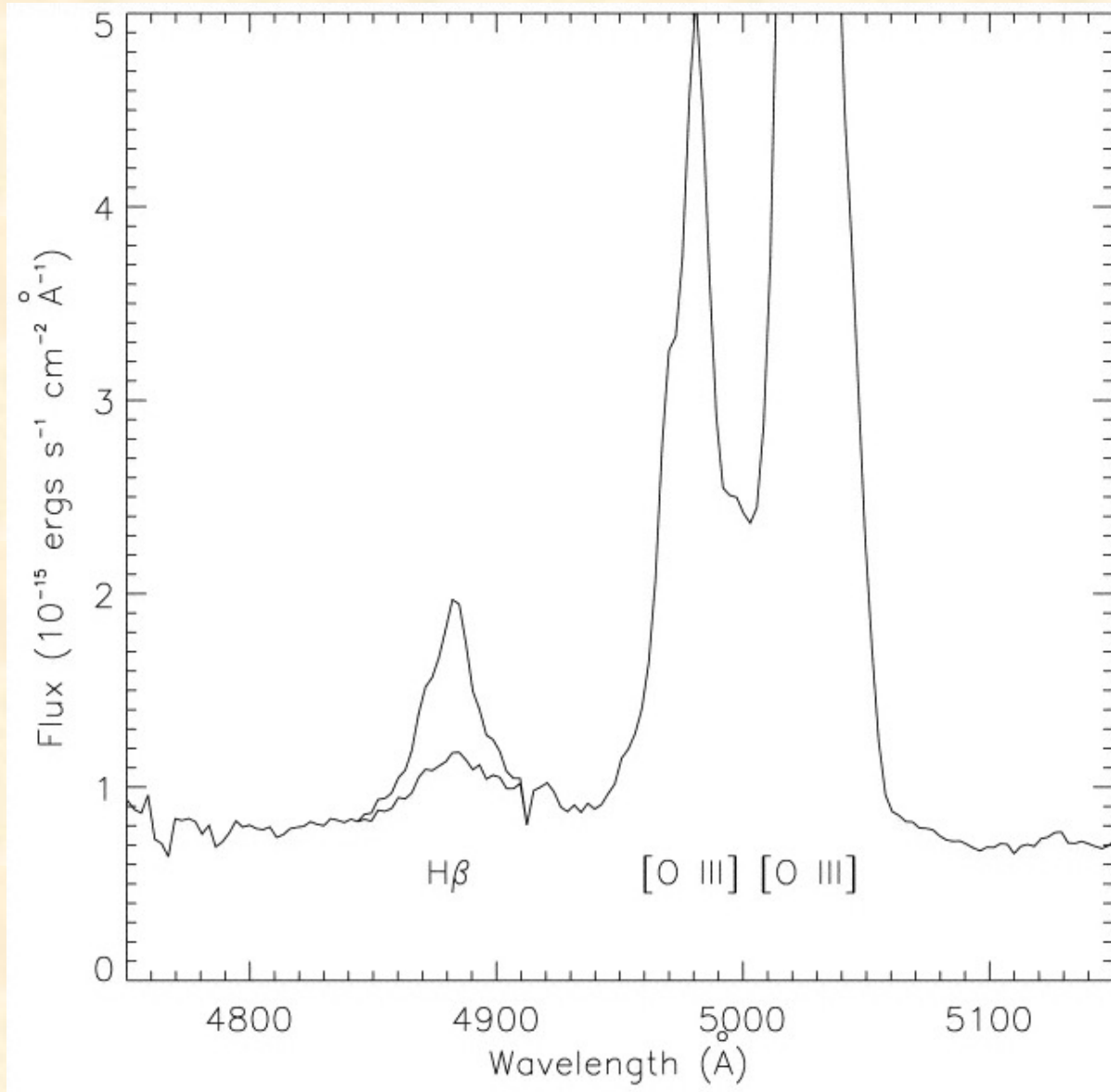


STIS UV Spectrum

(G140L; Crenshaw & Kraemer, 2000, ApJ, 532, 247)

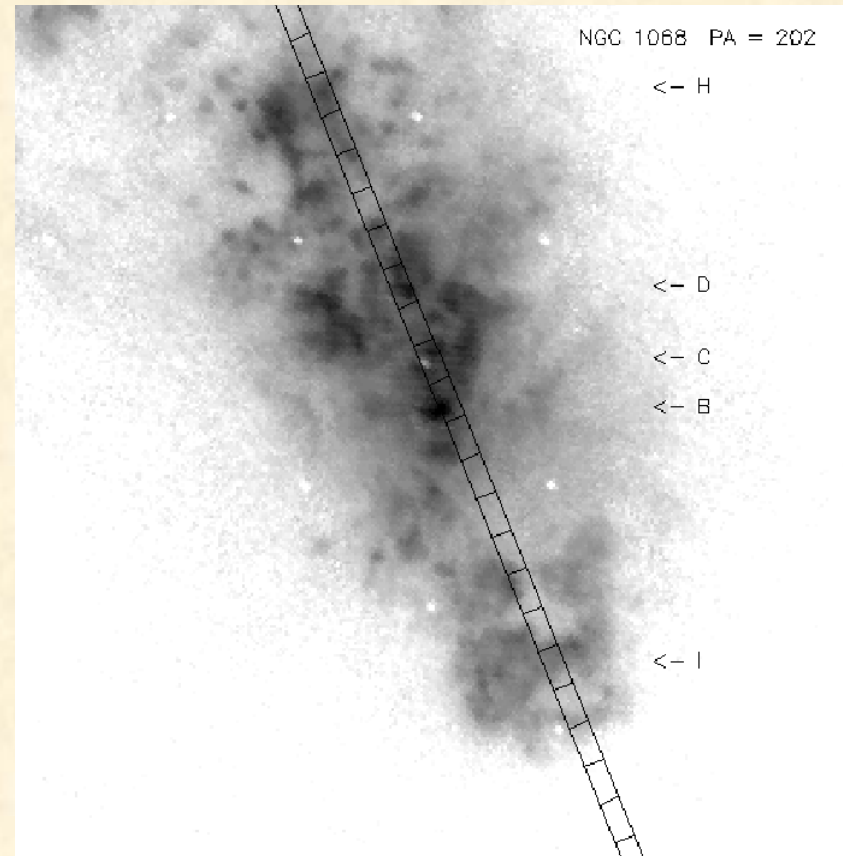
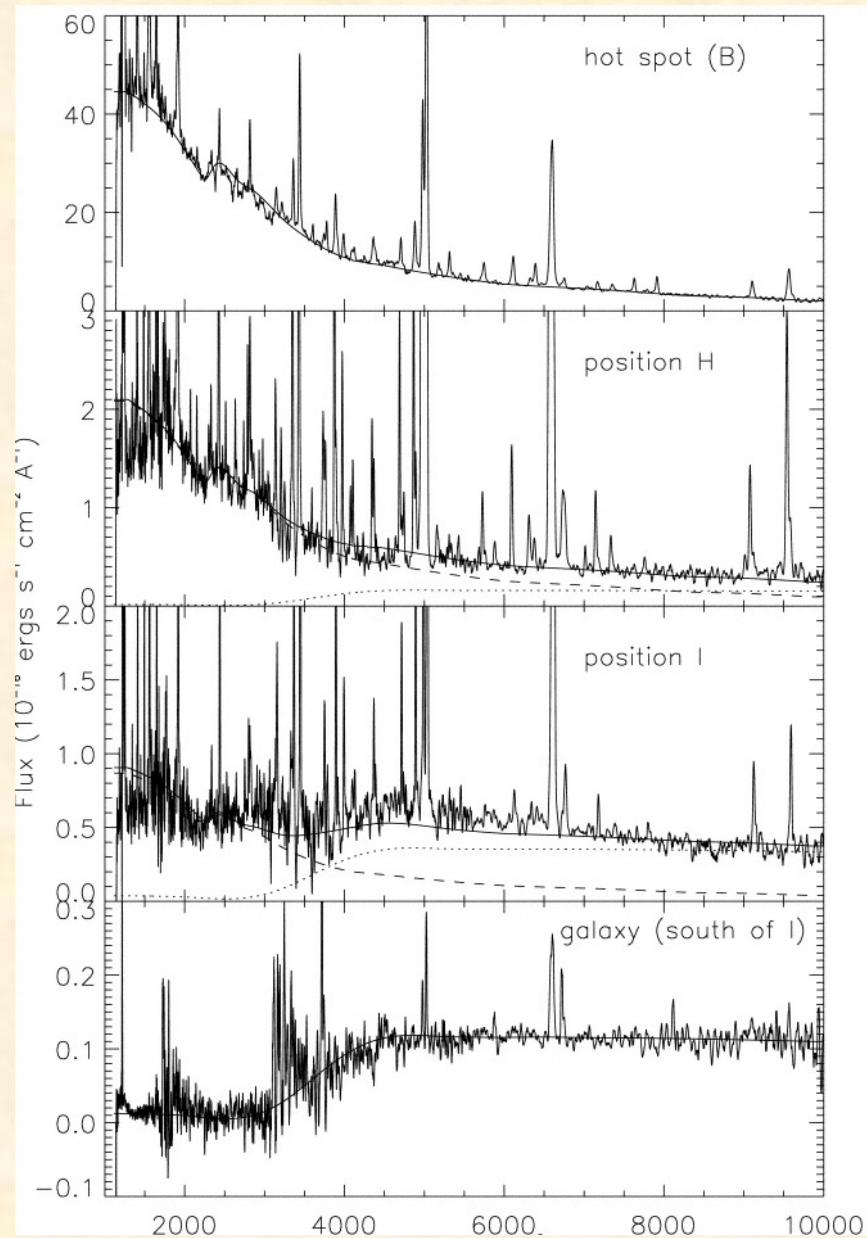


- hot spot is reflected continuum radiation



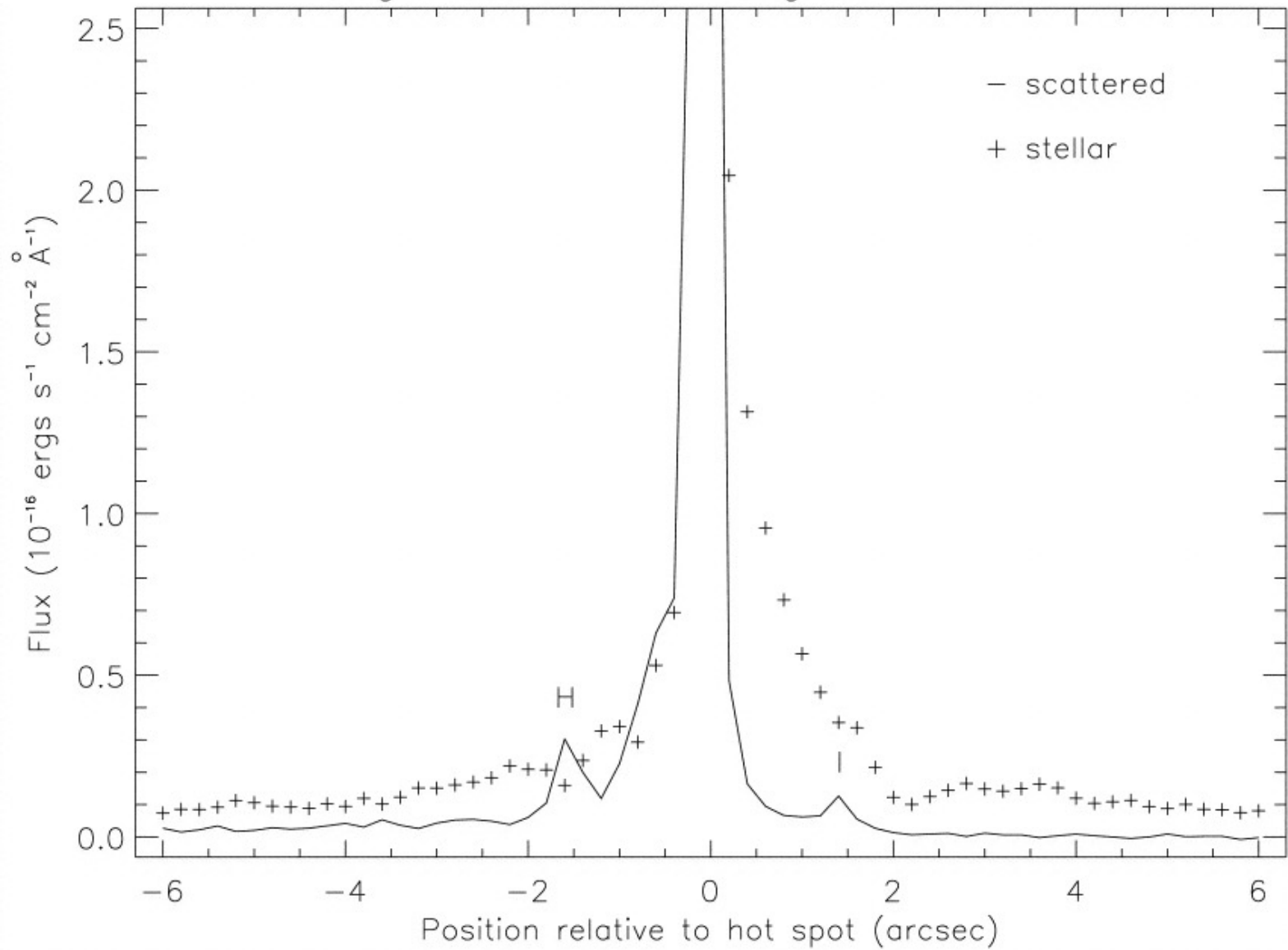
- Scattered BLR light seen directly

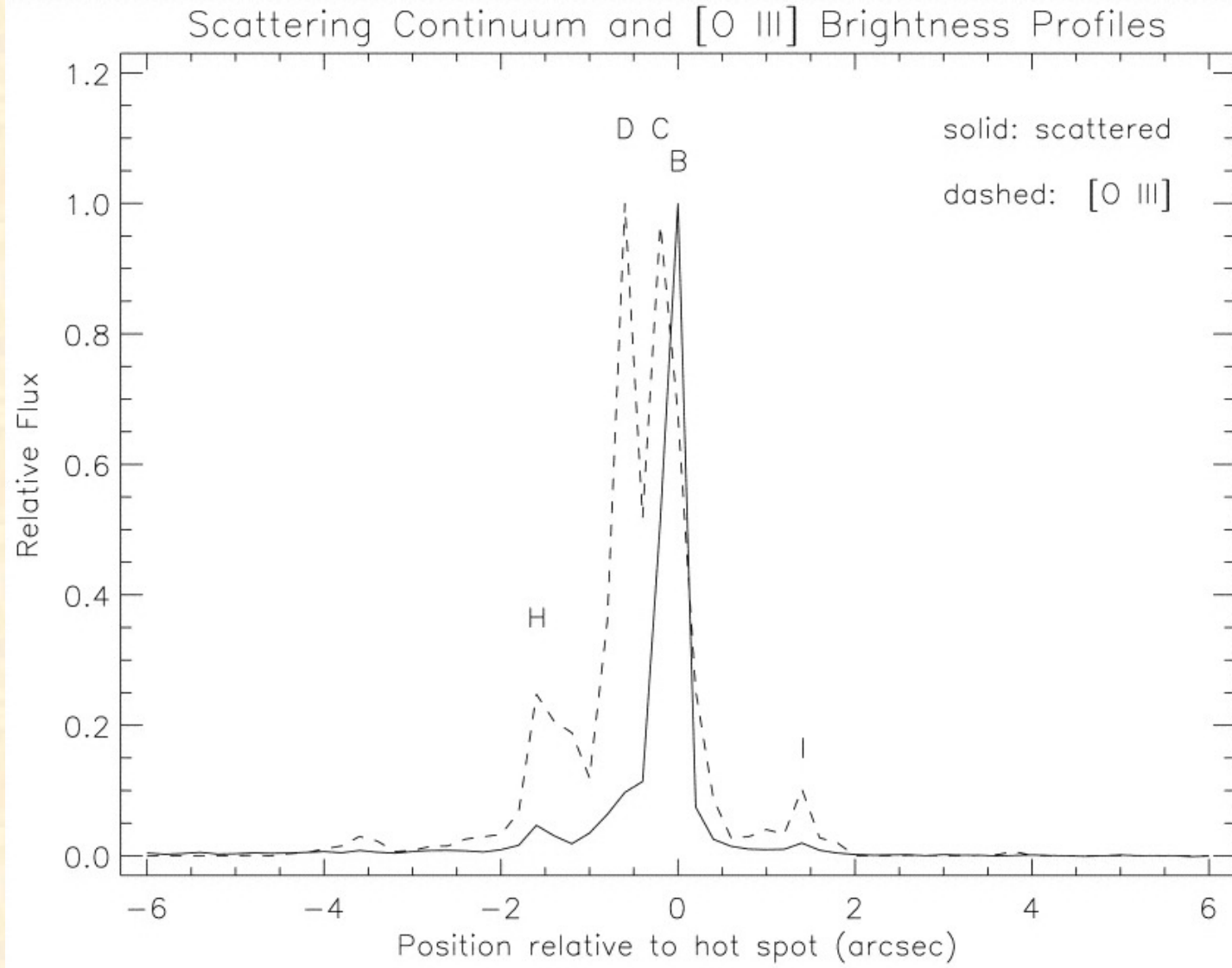
STIS Spatially-Resolved Spectra



Continuum at any position can be matched with a linear combination of reflected nuclear (dashed) and galaxy (dotted) spectra.

Brightness Profiles Along Slit at 5500 Å

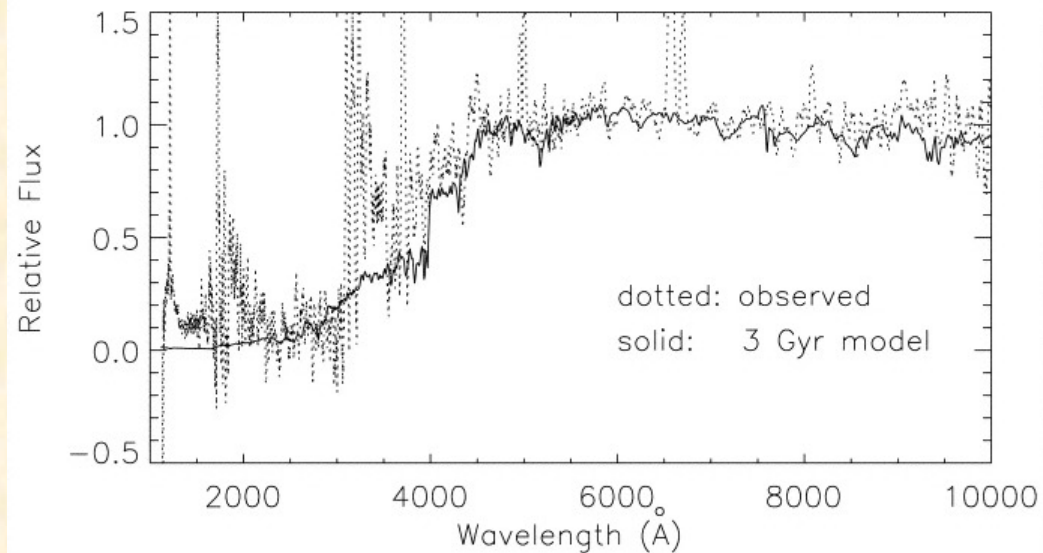
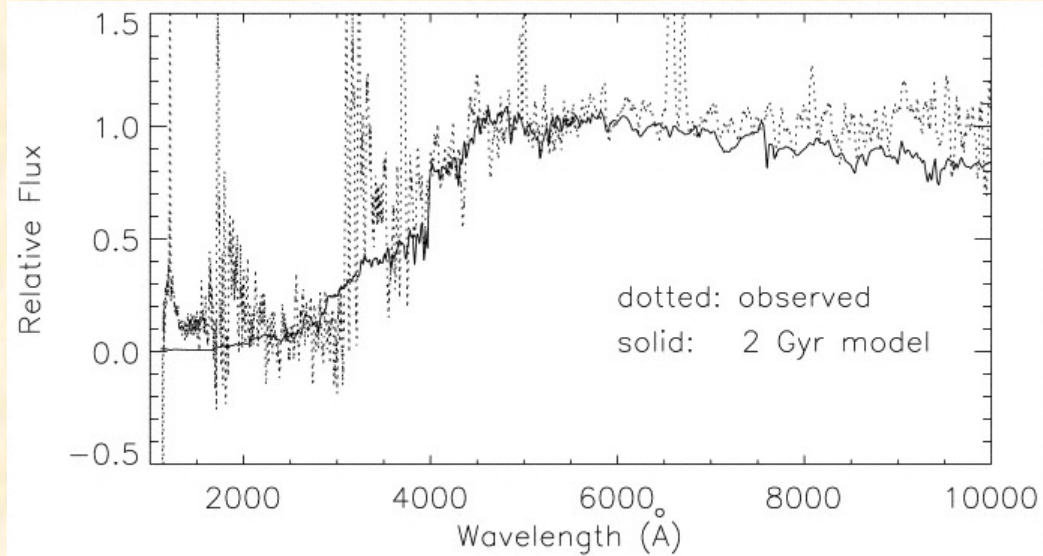




- regions of enhanced electron scattering are co-located with emission-line clouds.

Stellar Population Models

(Bruzual & Charlot, 1993, ApJ, 405, 538)

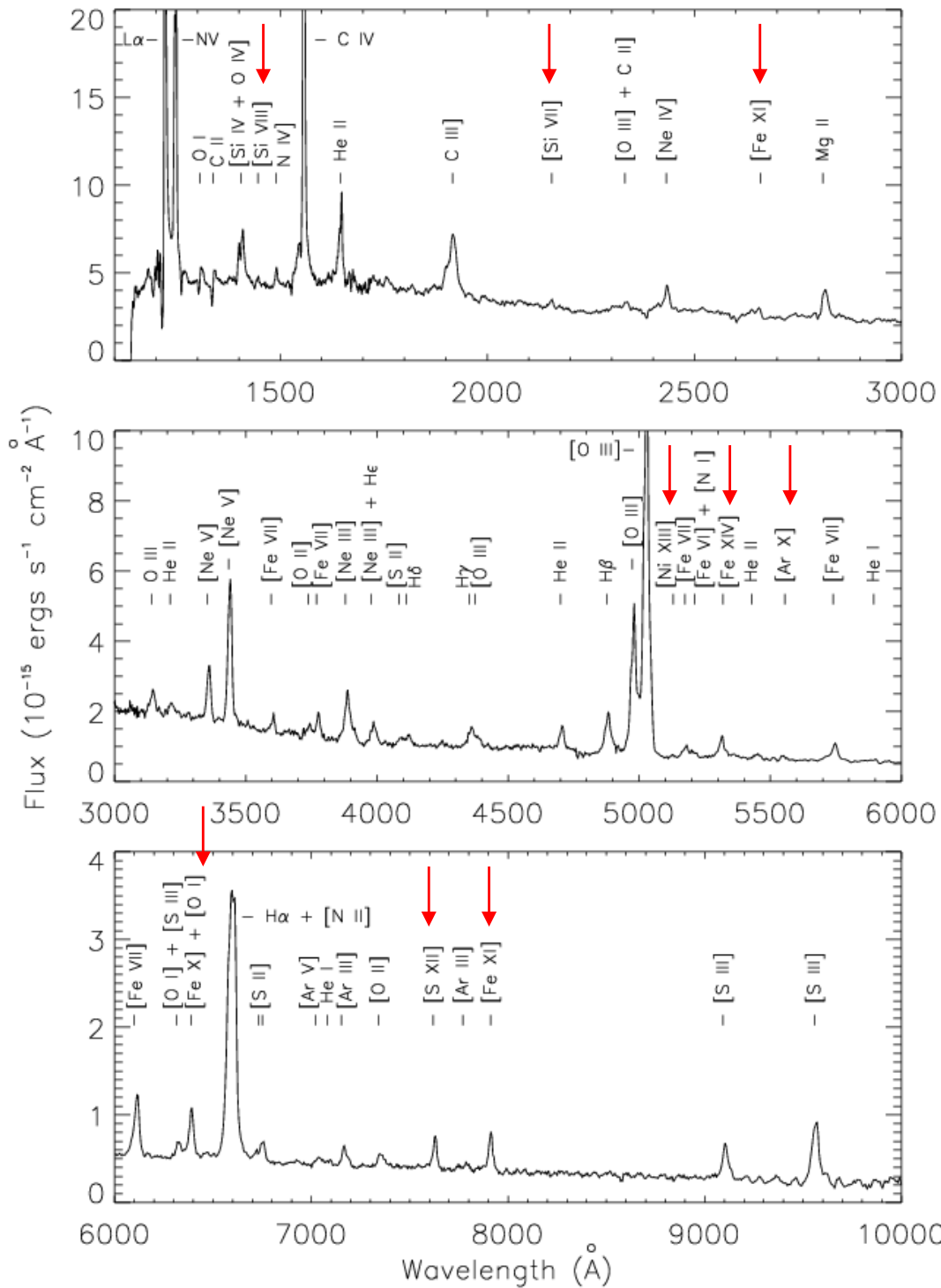


Age of nuclear cluster
Is 2 – 3 Gyr.

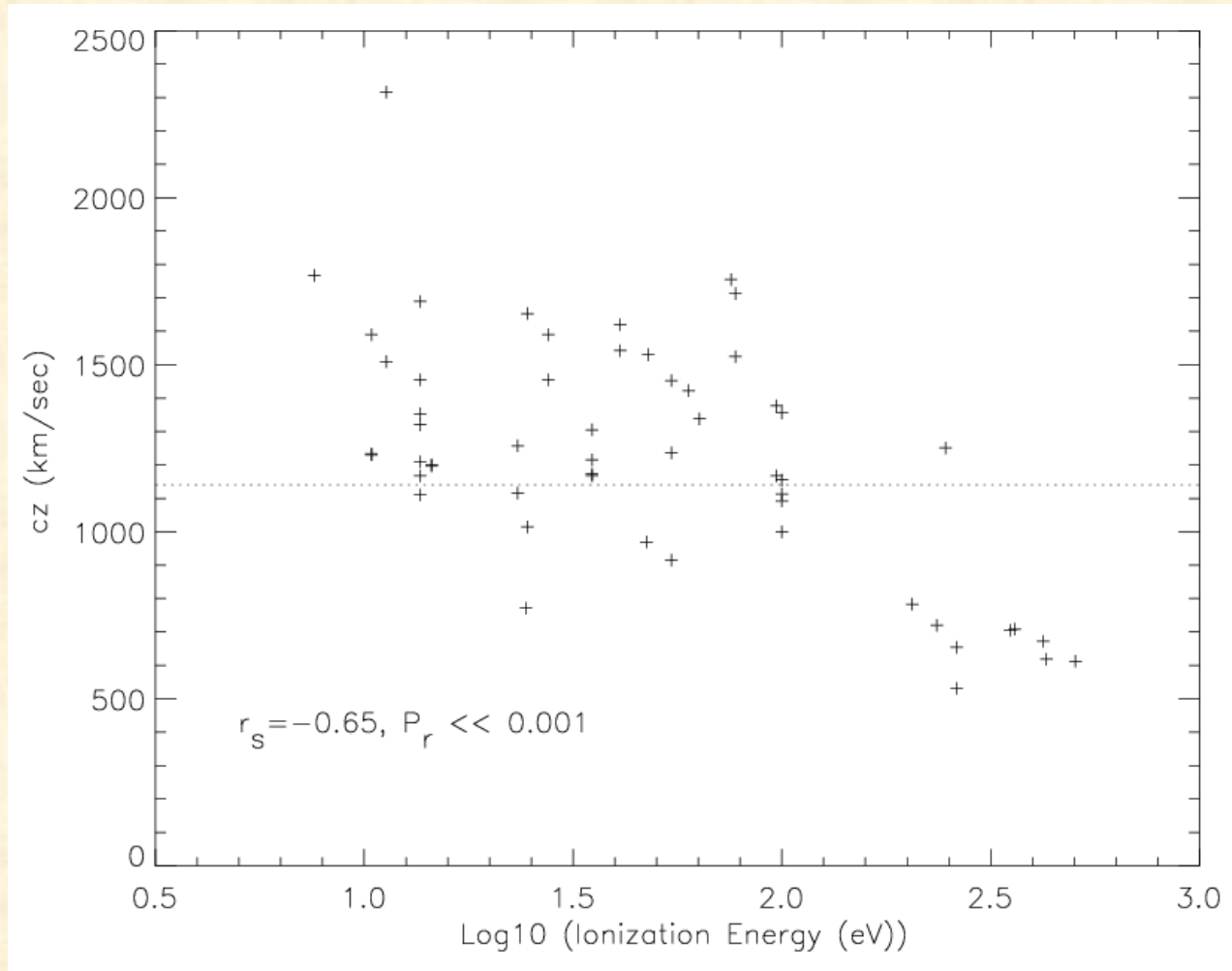
NGC 1068 Hot Spot: Physical Conditions (Kraemer & Crenshaw, 2000, ApJ, 532, 256)

Huge range in ionization:

- Low: O I, Mg II, C II
- High: C IV, [O III], etc.
- Coronal: [Fe XI], [Fe XIV], [S XII] ($IP_C = 504 \text{ eV}$)



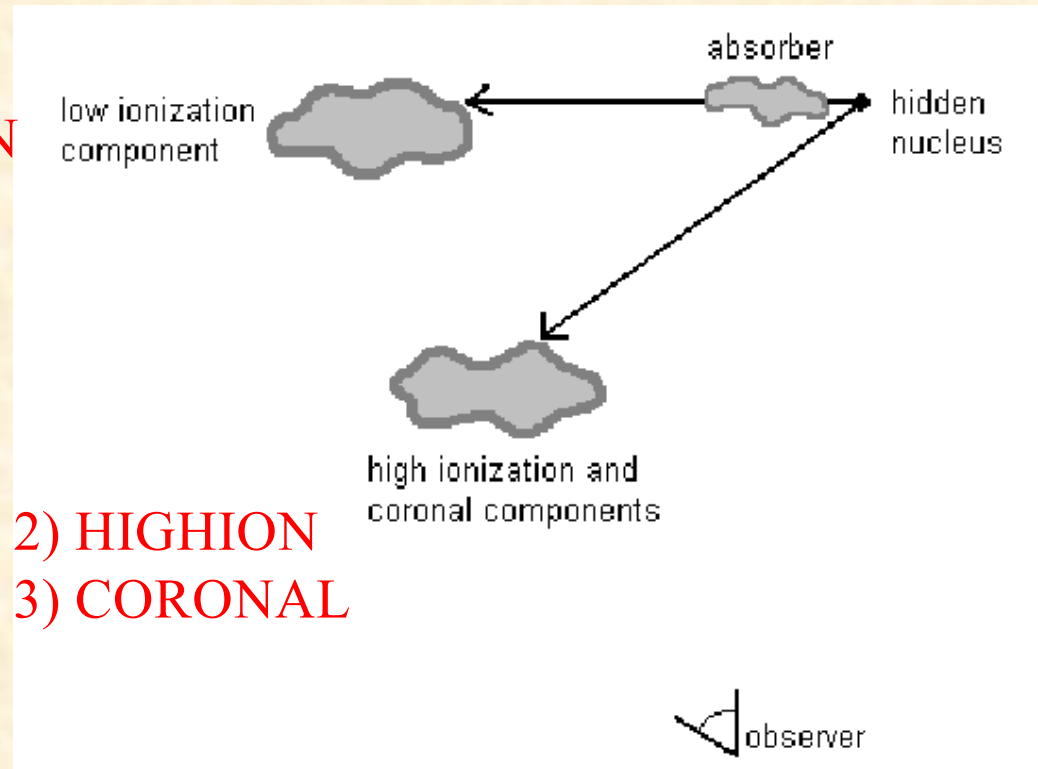
Redshift vs. Ionization Potential



-kinematic evidence for distinct components within the hot spot

NLR Photoionization Model – 3 components

1) LOWION



2) HIGHION

3) CORONAL

(Kraemer & Crenshaw, 2000, ApJ, 532, 256)

Component	U (ionization parameter)	n_H (number density, cm^{-3})	N_H (column density, cm^{-2})
LOWION	$10^{-3.2}$	3×10^4	1×10^{21}
HIGHION	$10^{-1.5}$	6×10^4	1×10^{21}
CORONAL	$10^{0.2}$	7×10^2	4×10^{22}

What can we learn from these studies?

- Distribution of physical conditions in the NLR
- Importance of dust and reddening in the NLR
- Total mass of ionized gas
- Importance of shocks vs. photoionization
- Information on the SED, particularly in the EUV.
- Ionization parameter, column \rightarrow Force multipliers for dynamical models using radiative driving
- Mass outflow rates and kinetic luminosities as a function of position in the NLR.